PENNSTATE

Applied Research Laboratory

FINAL REPORT

Grant No.: NAG2-1182

Condition Monitoring of Large-Scale Facilities

PREPARED FOR

NASA Ames Research Center

REPORT DATE

March 1999

POINT OF CONTACT

Dr. David L. Hall
Applied Research Laboratory
The Pennsylvania State University
P.O. Box 30
State College, PA 16804-0030
Telephone: (814) 863-4155
Fax: (814) 863-0673
E-mail: dlh28@psu.edu

Introduction

This document provides a summary of the research conducted under for the NASA Ames Research Center under grant NAG2-1182 (*Condition-Based Monitoring of Large-Scale Facilities*). The information includes copies of view graphs presented at NASA Ames in the final Workshop (held during December of 1998), as well as a copy of a technical report provided to the COTR (Dr. Anne Patterson-Hine) subsequent to the workshop. The material describes the experimental design, collection of data, and analysis results associated with monitoring the health of large-scale facilities. In addition to this material, a copy of the Pennsylvania State University Applied Research Laboratory data fusion visual programming tool kit was also provided to NASA Ames researchers.

NASA National Full-Scale Aerodynamic Complex

Fan Blade Integrity Research Feasibility Study Interim Report

PENNSTATE ARL

NFAC Facility

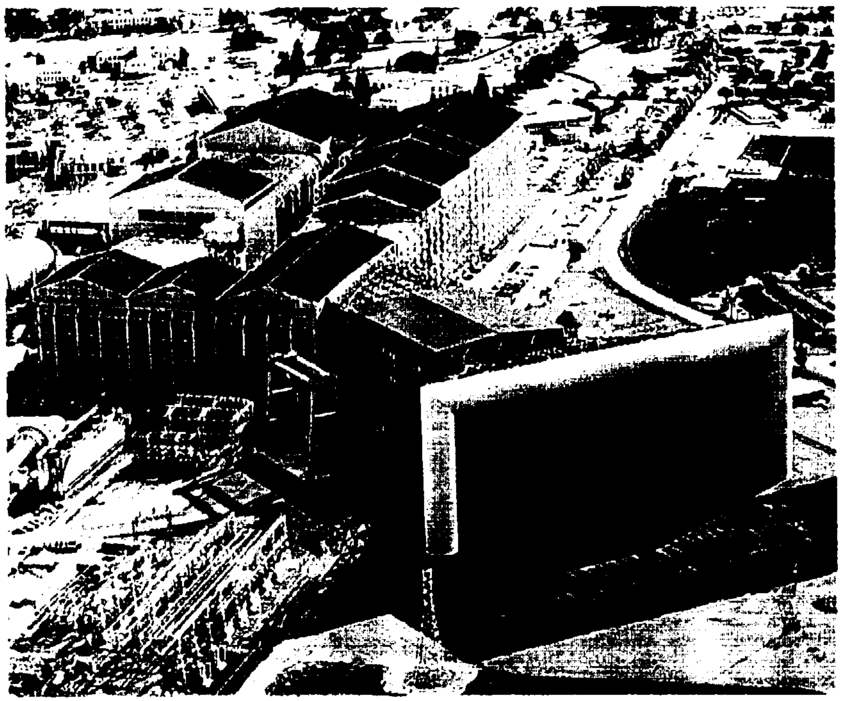

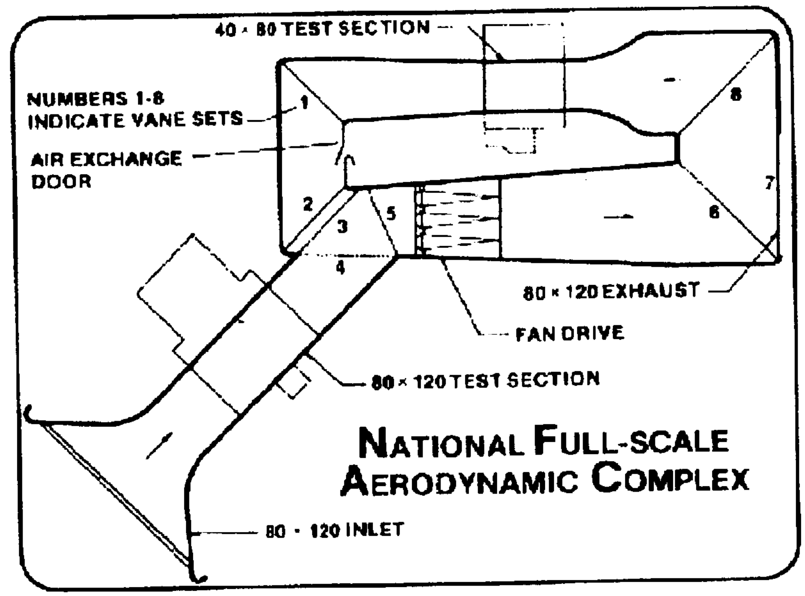

PENNSTATE ARL

The Fans

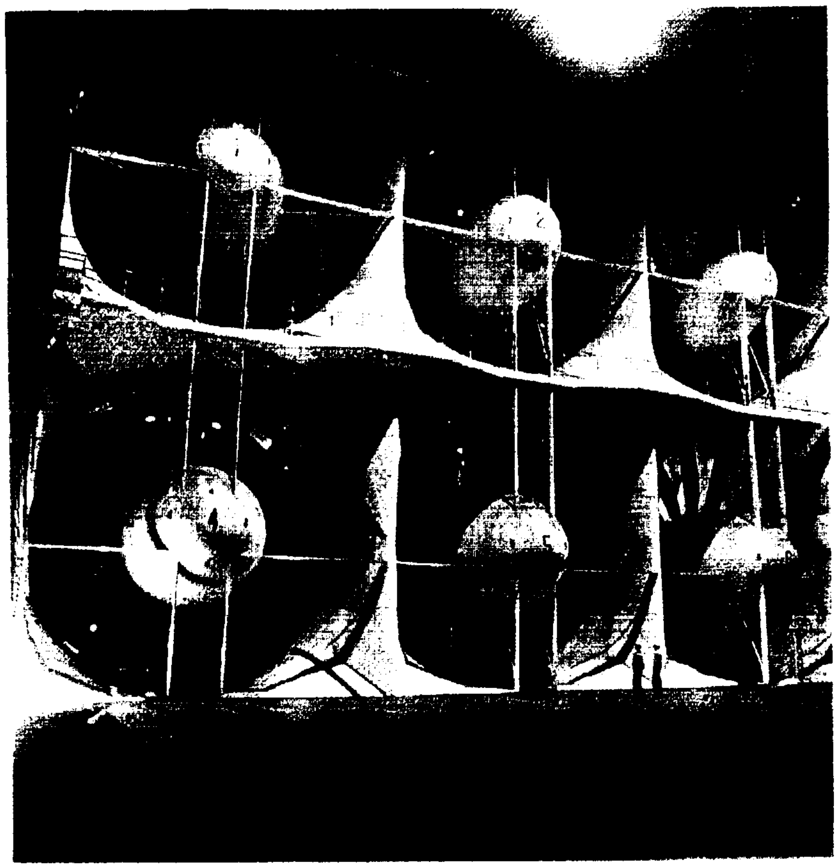

PENNSTATE ARL

The Issue: Fan Blade Integrity

- Assumption: Blade natural frequency shifts as crack begins to affect stiffness
  - Investigation of the validity is currently being performed by NASA Ames
  - High cycle, high level fatigue testing in progress
- Tracking blade natural frequencies currently involves impact testing of all 90 blades
- Desired: on-line, non-intrusive method for tracking of blade natural frequencies

The Solution: Detection of Blade Natural Frequencies in the Torsional Domain

PENNSTATE ARL

Instrumentation of Fan Shaft

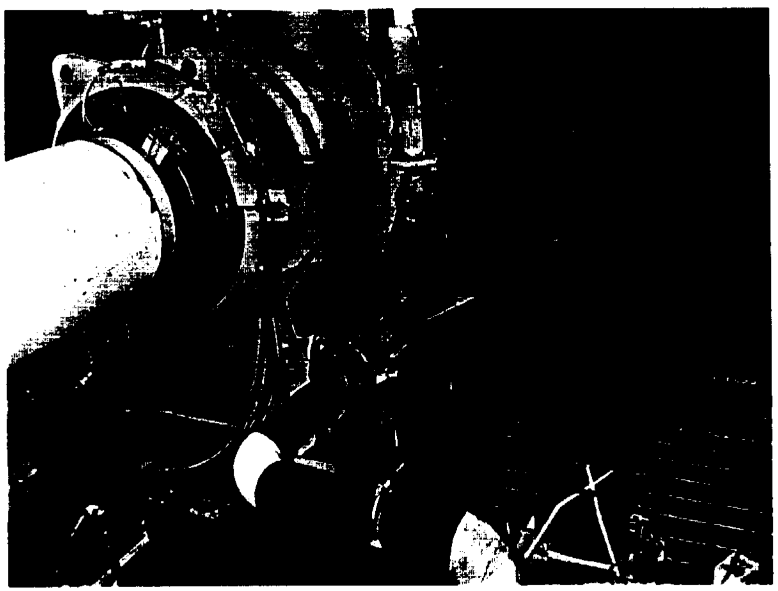

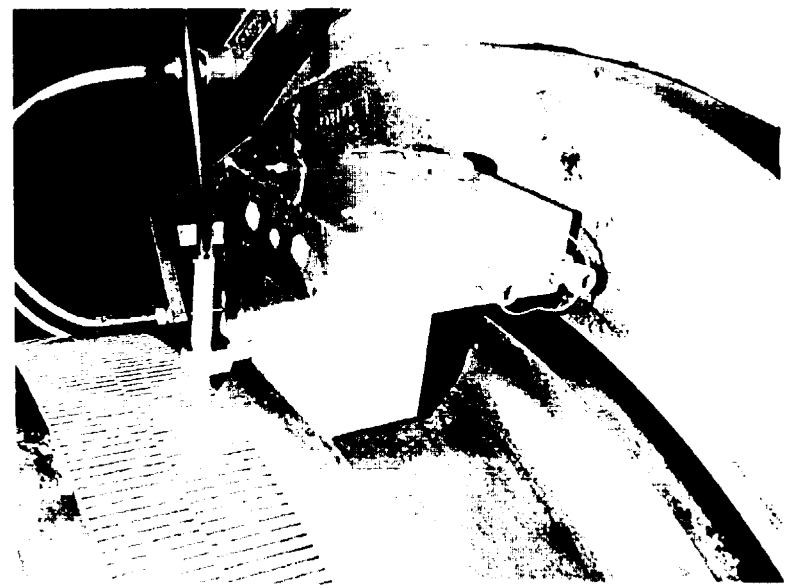

PENNSTATE ARL

Averaged Demodulated Spectrum (Preliminary Data Collection)

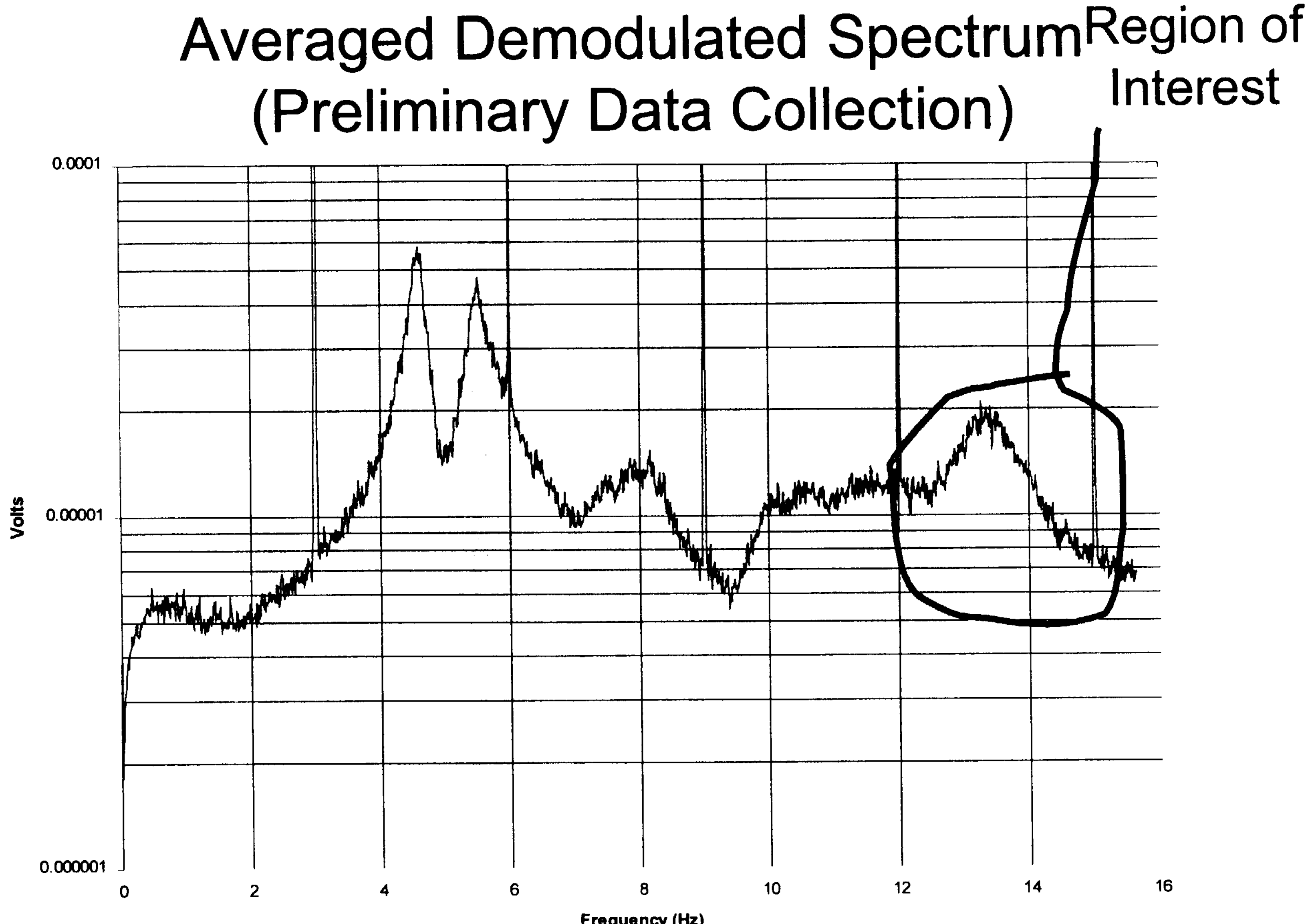

PENNSTATE ARL

Time Wave Form
(4096 points)

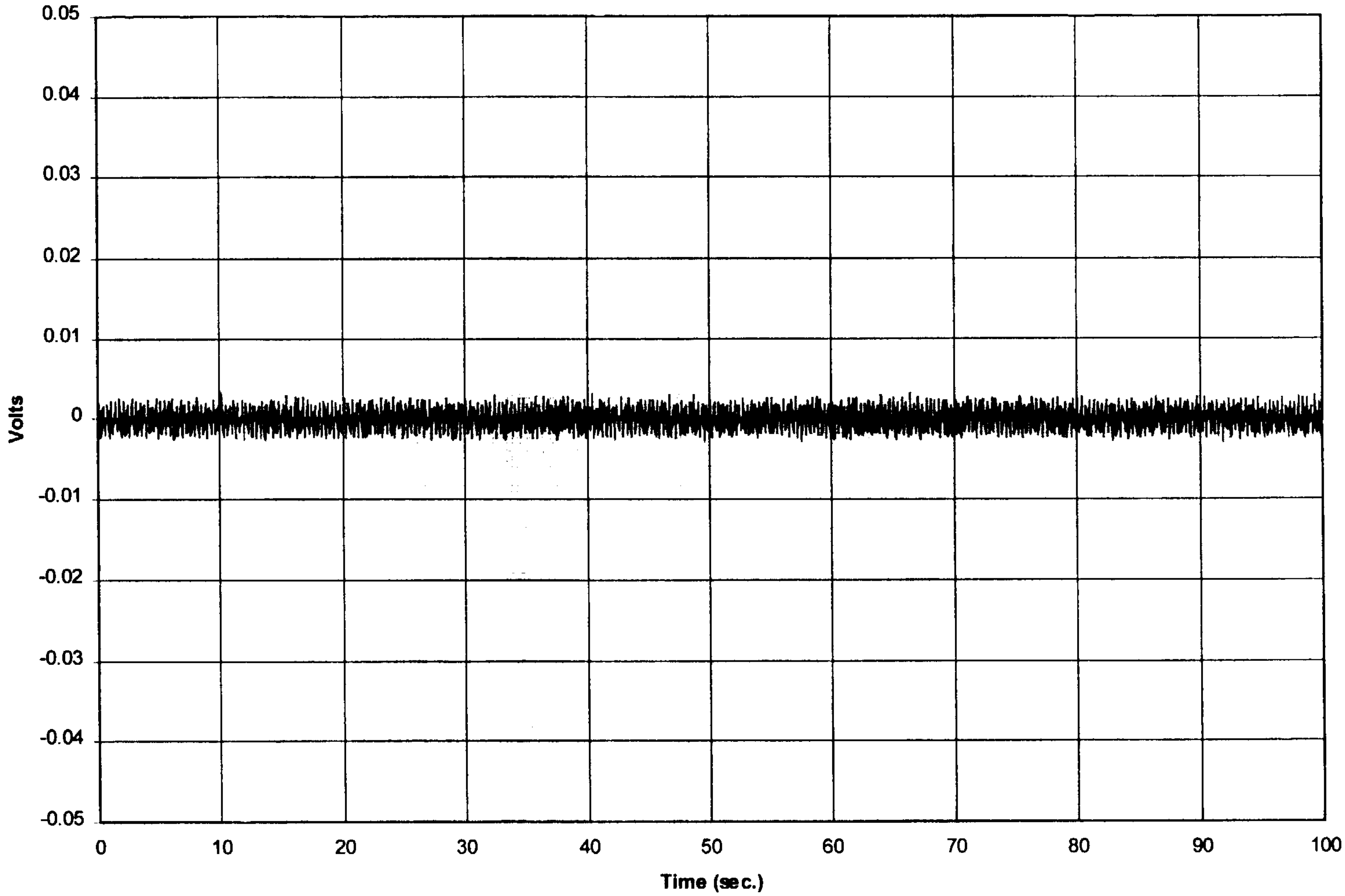

PENNSTATE ARL

Average Spectrum with Single Spectrum Overlay of 4096 Points

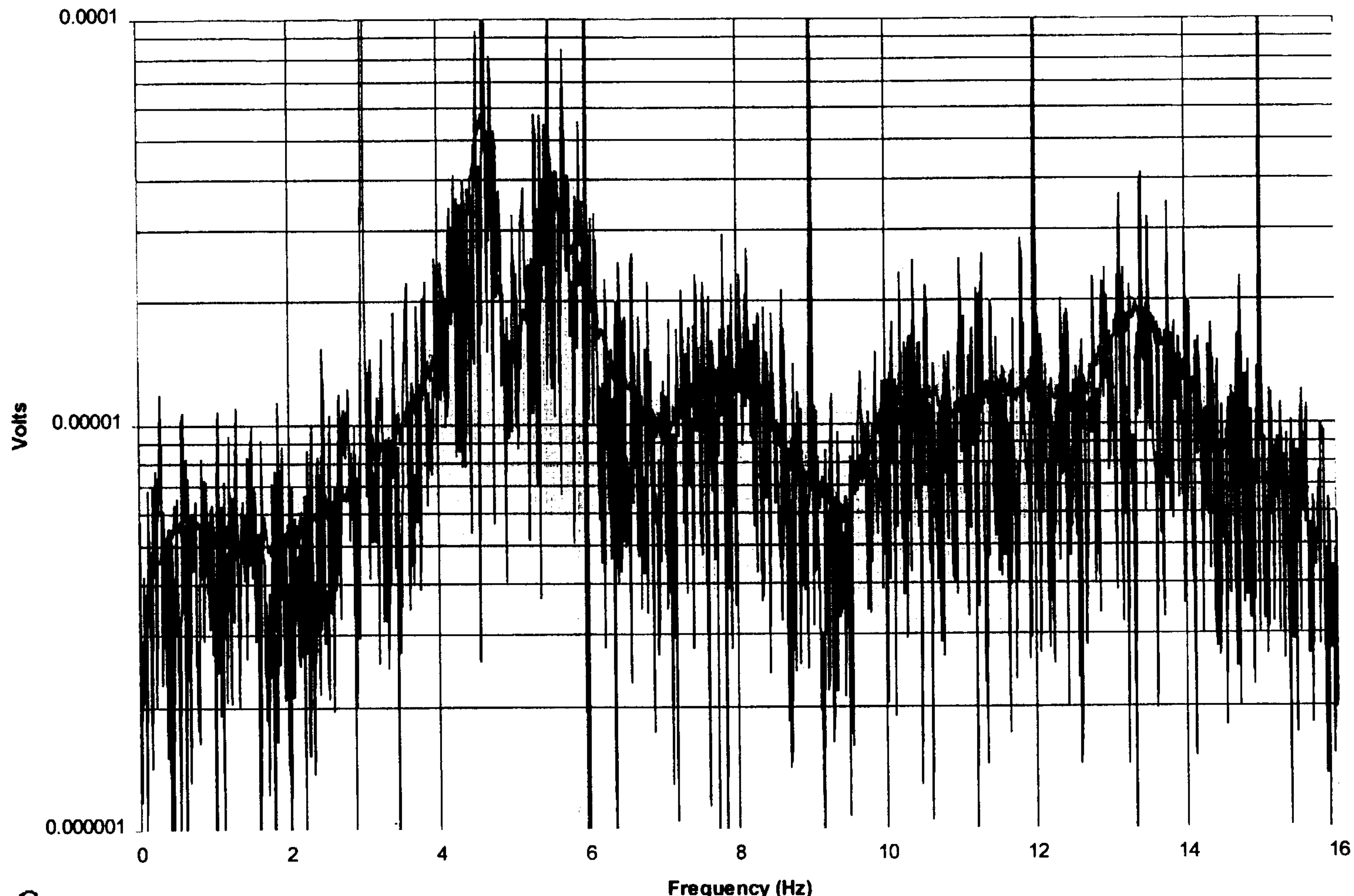

PENNSTATE ARL

Modal Impact Test

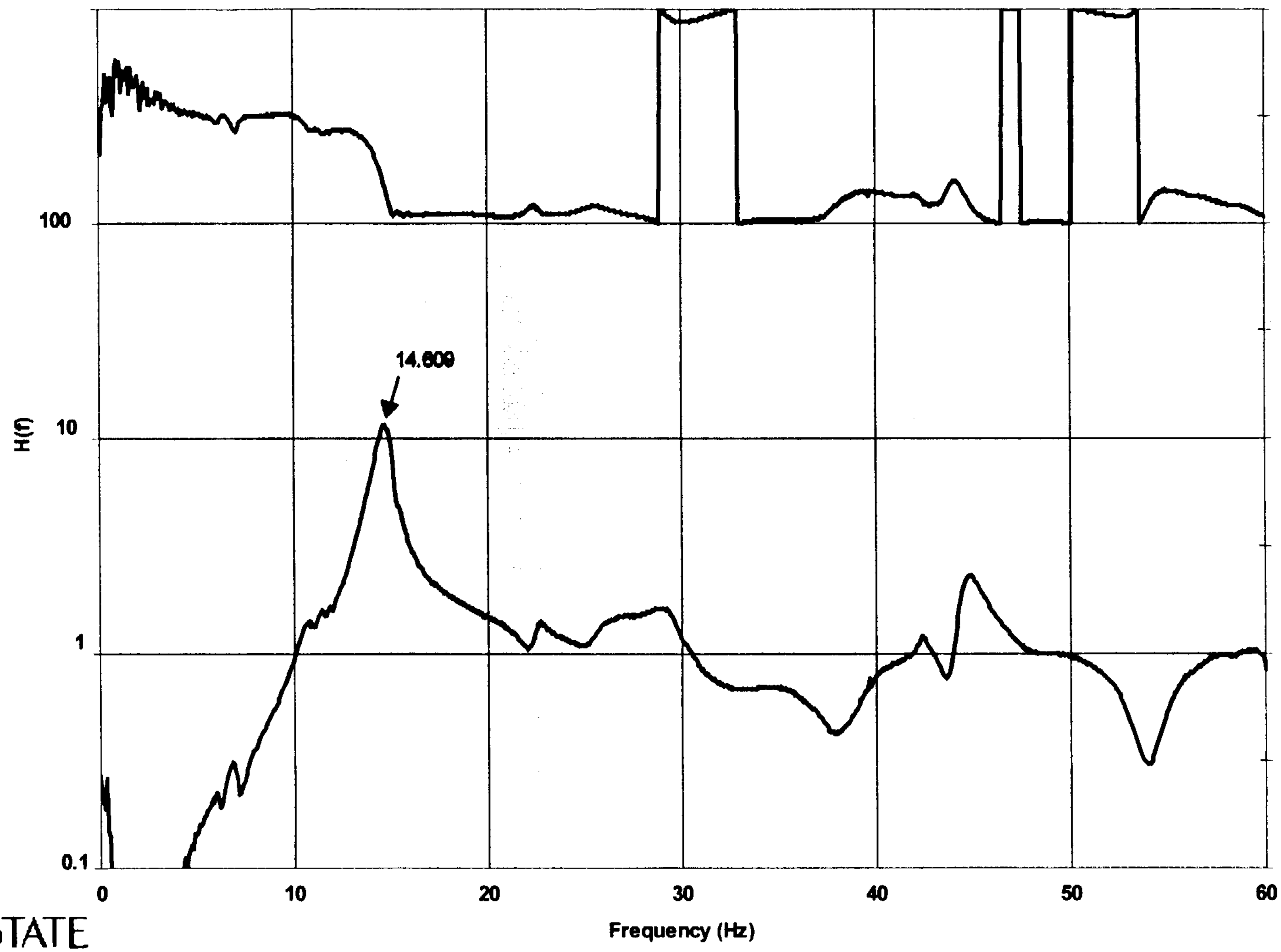

PENNSTATE ARL

Remaining Feasibility Study Tasks

- Obtain significant block of high dynamic range data
- Compare effectiveness of digital signal processing algorithms for extraction of blade natural frequencies:
  - Fast Fourier Transform and Zoom FFT techniques
  - Average Chirp-z
  - Wavelet de-noising
  - Filtering
  - Maximum Entropy Spectral Analysis (future)

PENNSTATE ARL

Future Research

PENNSTATE ARL

Long-Term Research Goals

- Conversion of demodulation process to digital (currently sponsored by Southern Company)
- Tape error and end effects compensation (currently sponsored by Southern Company)
- Optimizing transduction
  - single fiber probe
  - dual beam laser
  - two channel fiber optic system w/ interferometer
- Development of NFAC blade frequency detection system
- Demonstration of turbine blade frequency detection on actual turbine
- Shaft crack detection research for vertical pump

PENNSTATE ARL

Improved A/D and DSP

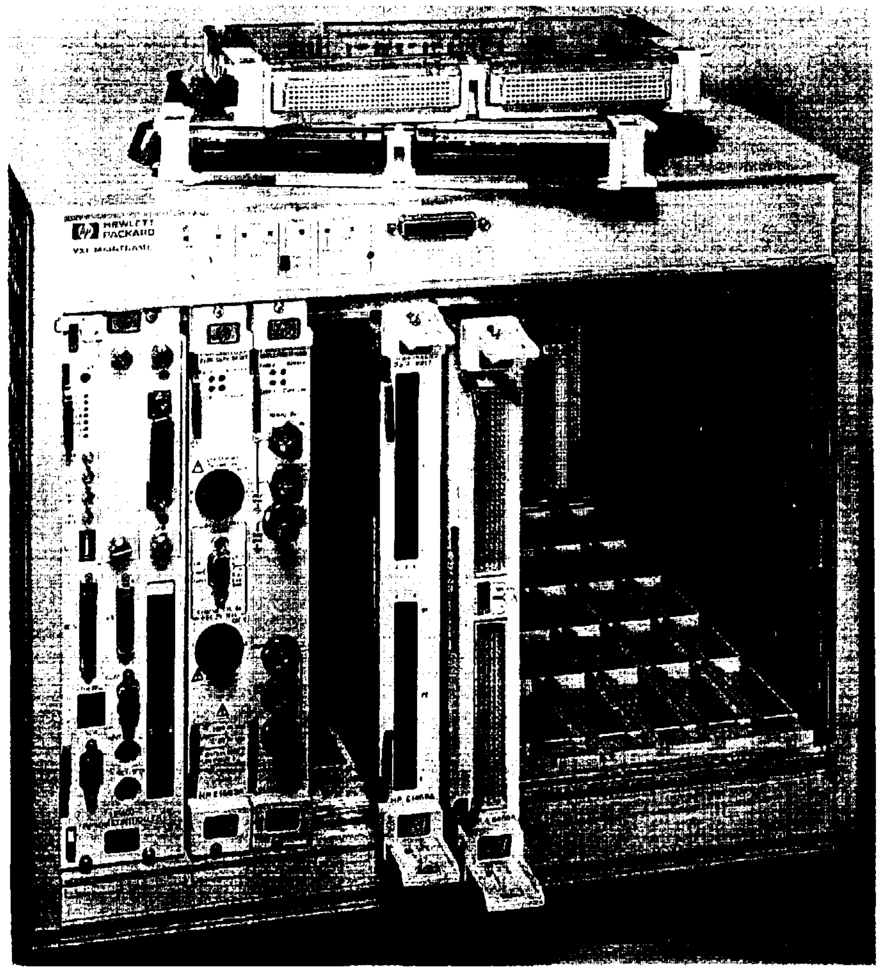

PENNSTATE ARL

The HP E1437A Card

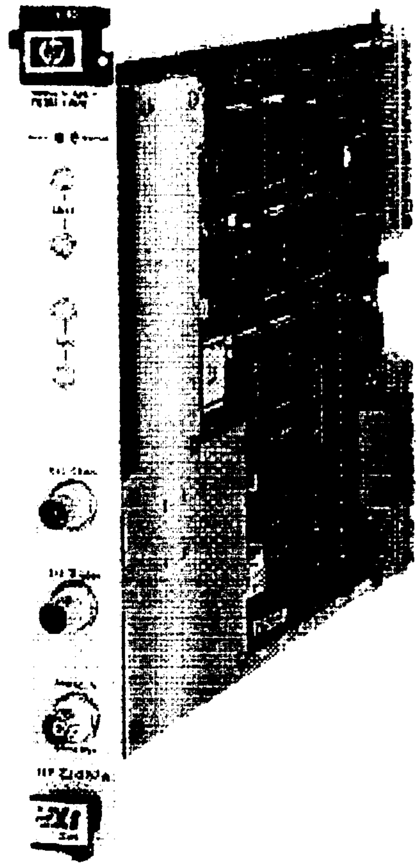

- 23-bit Sigma Delta A/D (>110 dB dynamic range)
- 20 MSa/sec. ADC
- 8 MHz Frequency Usable Band

PENNSTATE ARL

PENNSTATE

ARL

CBM Department

NASA / PSU Workshop

Data Acquisition & Statistical Signal Processing

By Derek C. Lang

Sept. 10-11, 1998

PENNSTATE ARL

Outline

- Data Acquisition System for FML
- Signal Processing / Statistical Analysis of MDTB Data
- Multi-Sensor Fusion Toolkit
- Future Work

PENNSTATE 1855 ARL

NASA Ames Research Center

FML Hitachi Speed Increaser

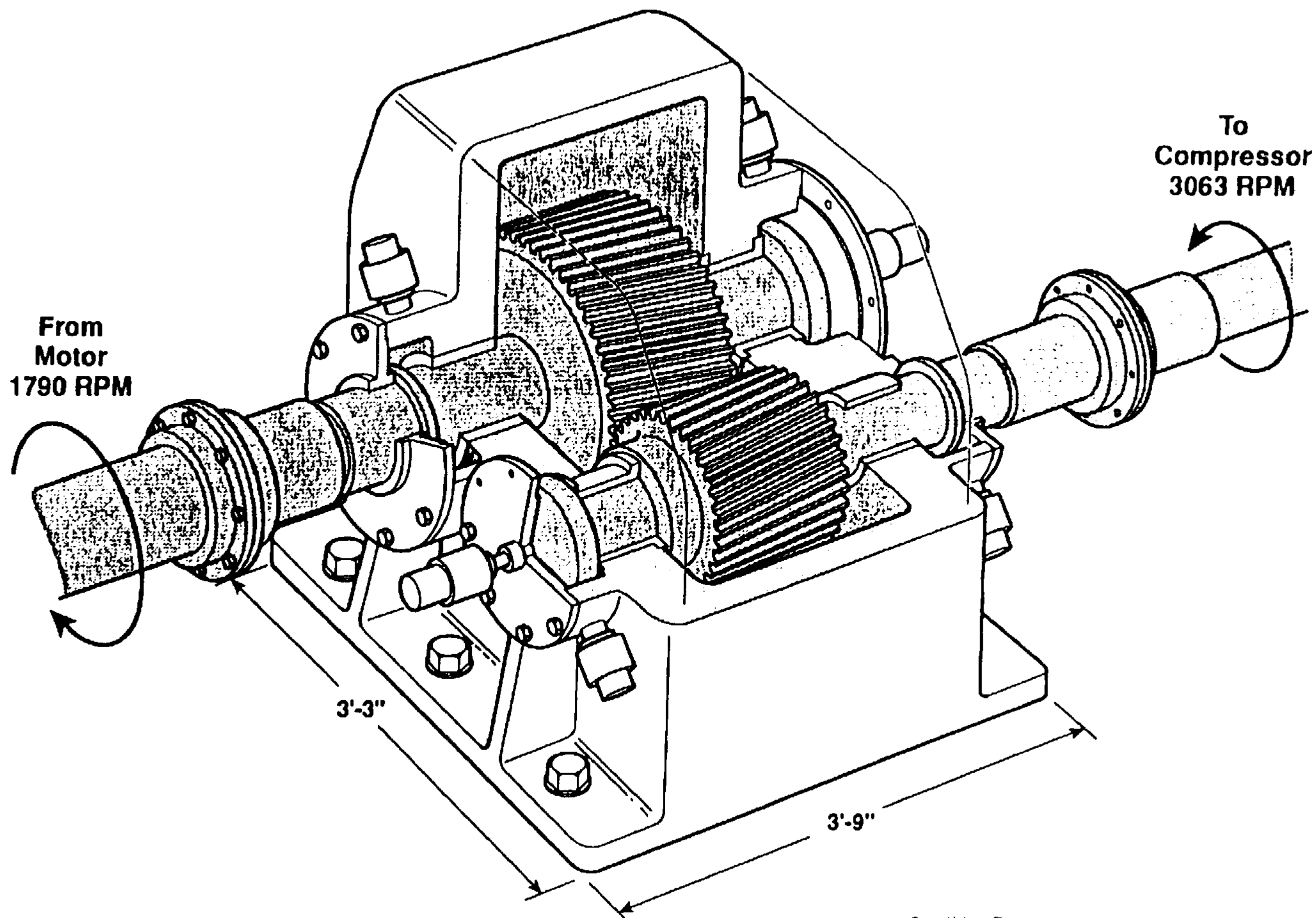

Condition Based Maintenance Program
Fluid Mechanics Laboratory

PENNSTATE

ARL

Monitoring Approach

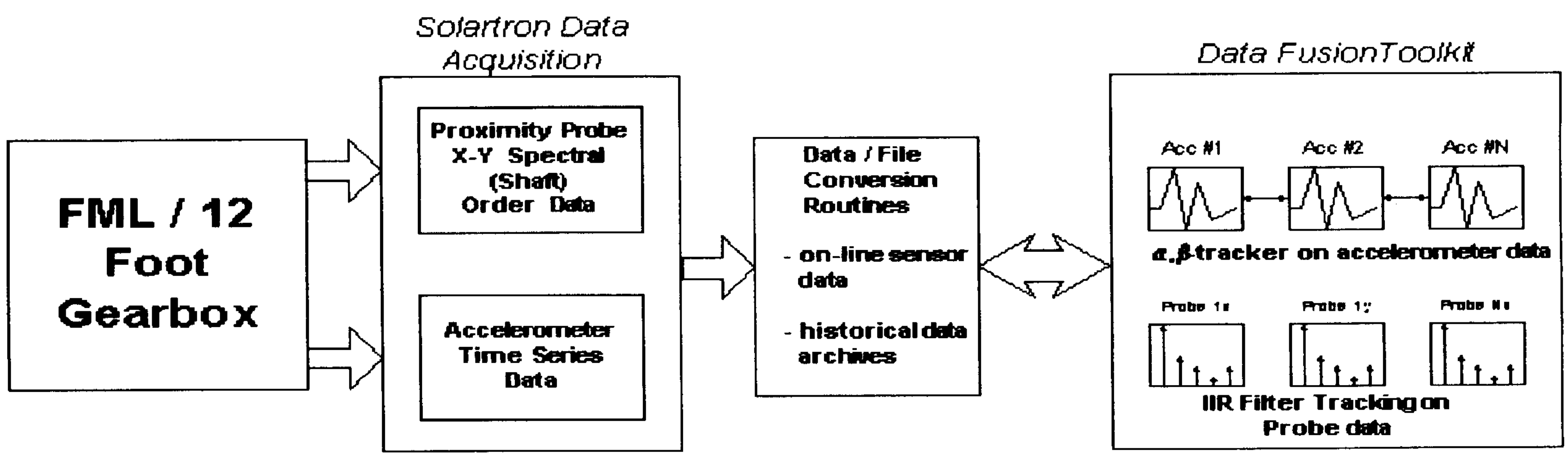

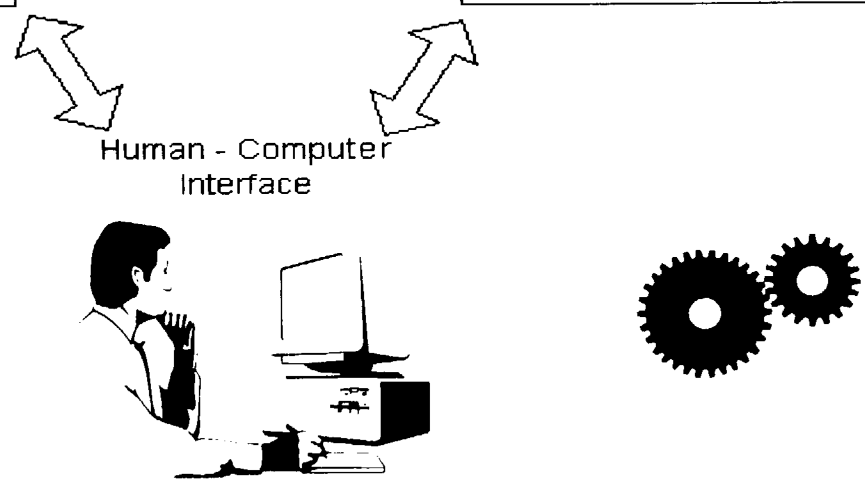

- DF Tool will trend data and display information with existing Solartron TS/Prox Probe outputs
- Visual C++ / Windows Interactive Environment
- Expandable Capability

Trending Requirements

- **Data Types:** Currently Working with Order Spectra and some Time Series Snapshots
- **Machine States:** Need to trend in Run-up / Steady State / Coast-Down
- **Accelerometer Time Series:**
  - Run Up (0 - 29 Hz.): 17 sec block
  - Steady State (approx. 29 Hz.): 10 sec block / 15 min.
  - Coast Down : 4 (10 sec blocks)
- **Proximity Probes:**
  - Run up / Steady State / Coast Down
- **Thresholds:**
  - Alert: 50% of current
  - Alarm: 100-200% of Current
  - OEM recommendations ?

DAQ2 Data Acquisition Process Flow

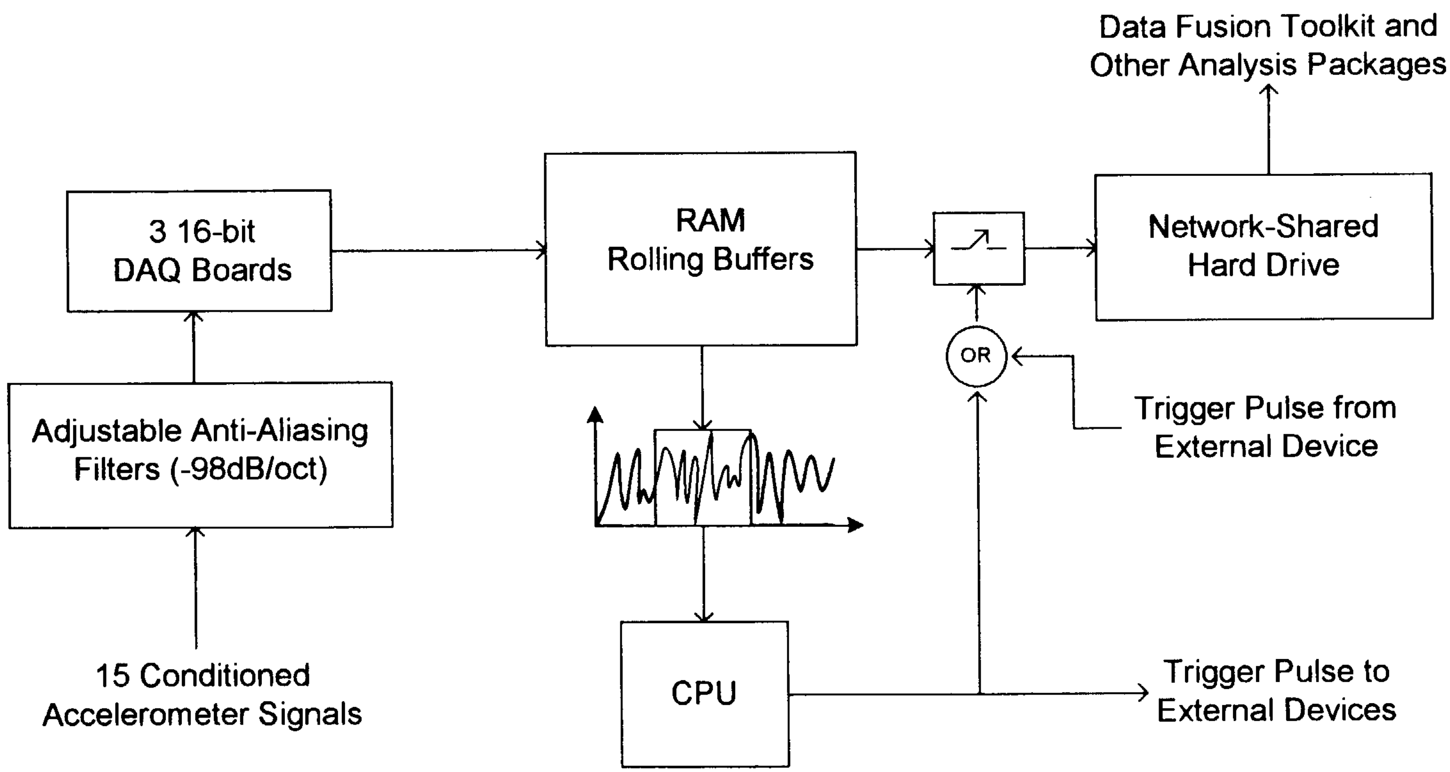

PENNSTATE

ARL

Key Features of Data Acquisition Setup

- Flexible Configuration
- Up to 75 triggers: RMS, FFT, Wavelet IIR, Time
- Data Saving, Emailing and/or Paging on Trigger Events
- Online Trigger Level Trending
- Monitor Program Checks/ Maintains DAQ's and Disk Space

- Programs are Multi-Threaded
- External DAQ & Data Synchronization
- Modular Program Setup for Easy Expansion of Triggers, DAQ's, etc.
- Network Linked Monitor to Insure System Operation

PENNSTATE

ARL

DAQ Program Settings & Control

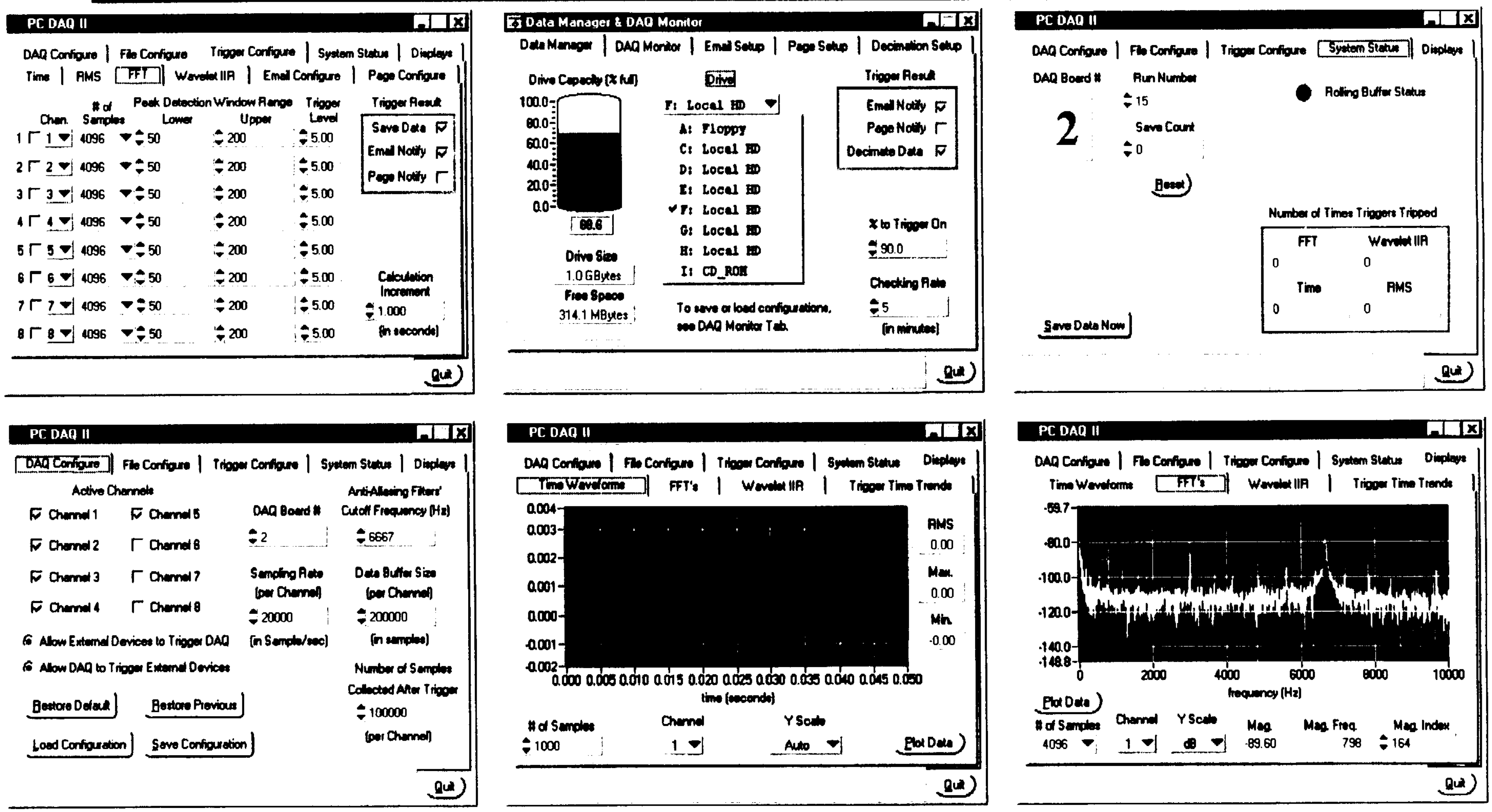

NASA Ames: FML DAQ 2
Data Acquisition Programs

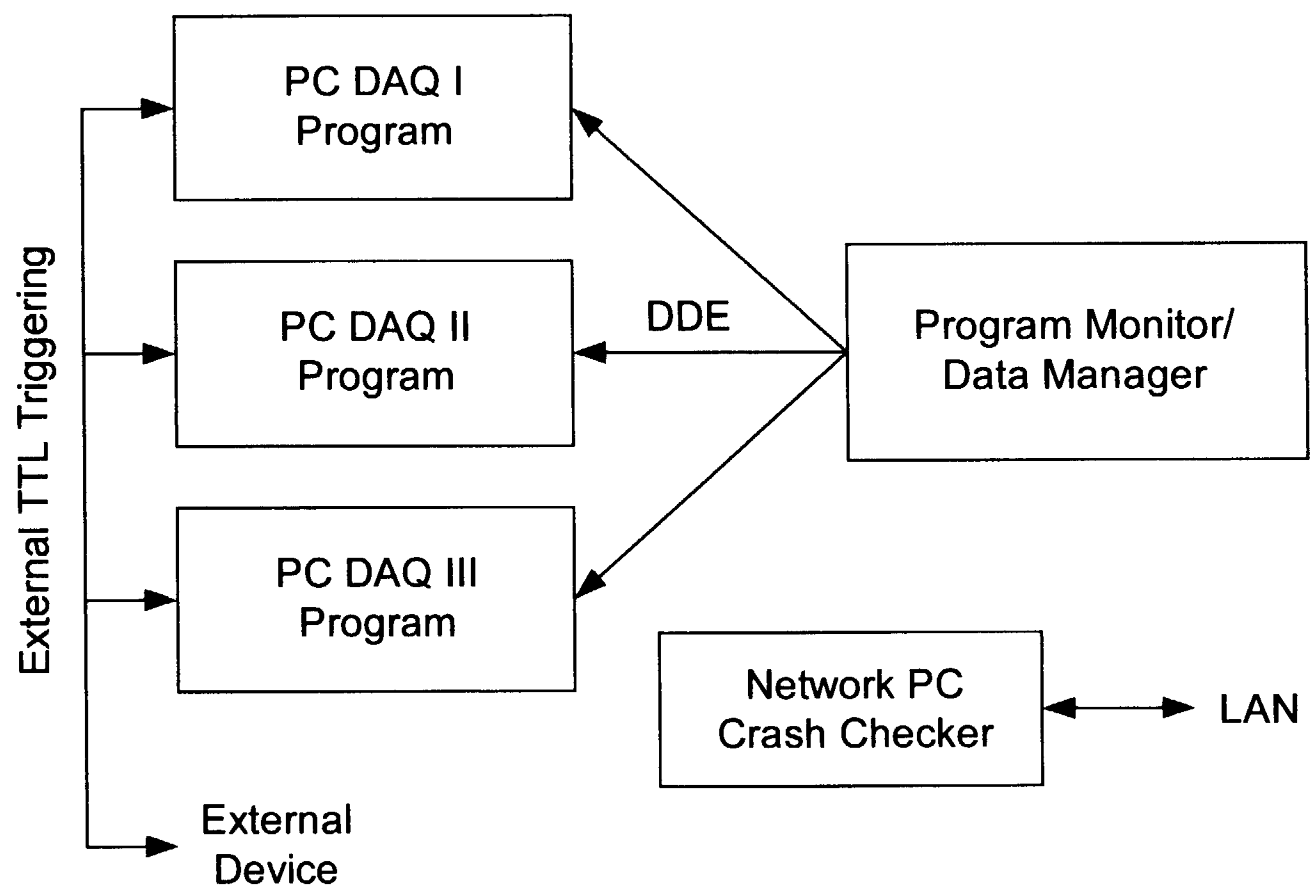

NASA Ames FML
DAQ2 File Format

Headers

ICHM Format

Offset	Comment	Offset	Record Length	Offset	Resolution
0	See Commets Tab	268	200000	278	16
	GMT Time		Data Type		Calibration
256	HHMMSS	272	1	280	0
	GMT Sec		Sample Size		Reserved
260	second clock	274	2	282	0
	GMT Date		Number Channels		Sample Rate
264	YYYYMMDD	276	1	284	20000

PENNSTATE

ARL

MDTB Run 14

Wavelet Trigger Shut-down 8:00 AM

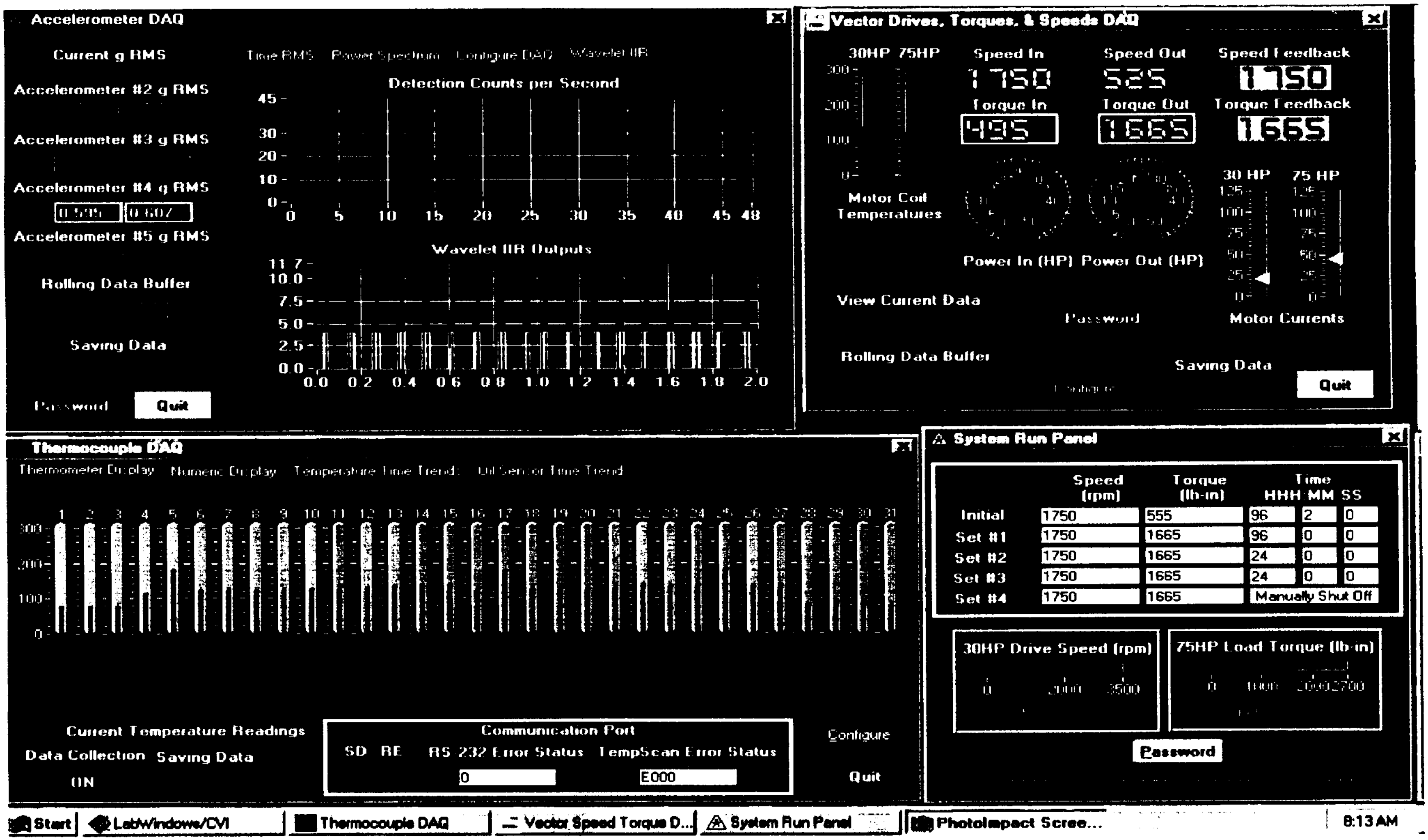

Continuous Wavelet Transform

- **Continuous Wavelet Transform**

$$C(a,b) = \int_{-\infty}^{\infty} \frac{1}{\sqrt{a}} s(t) \Psi\left(\frac{t-b}{a}\right) dt$$

- **Complex Morlet Wavelet**

$$\Psi(t) = e^{-j\omega_0 t} e^{\frac{-t^2}{2}} \qquad \omega_0 = 5$$

Complex Morlet Wavelet

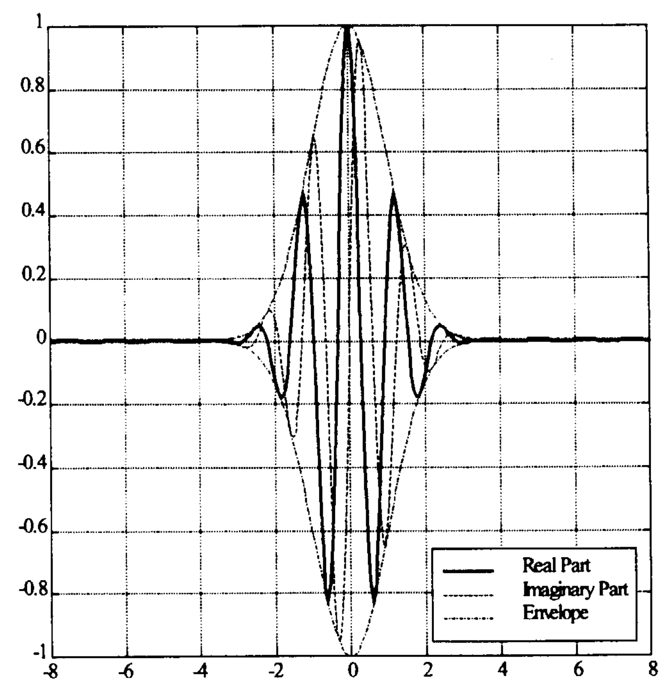

Wavelet
% Warning Times

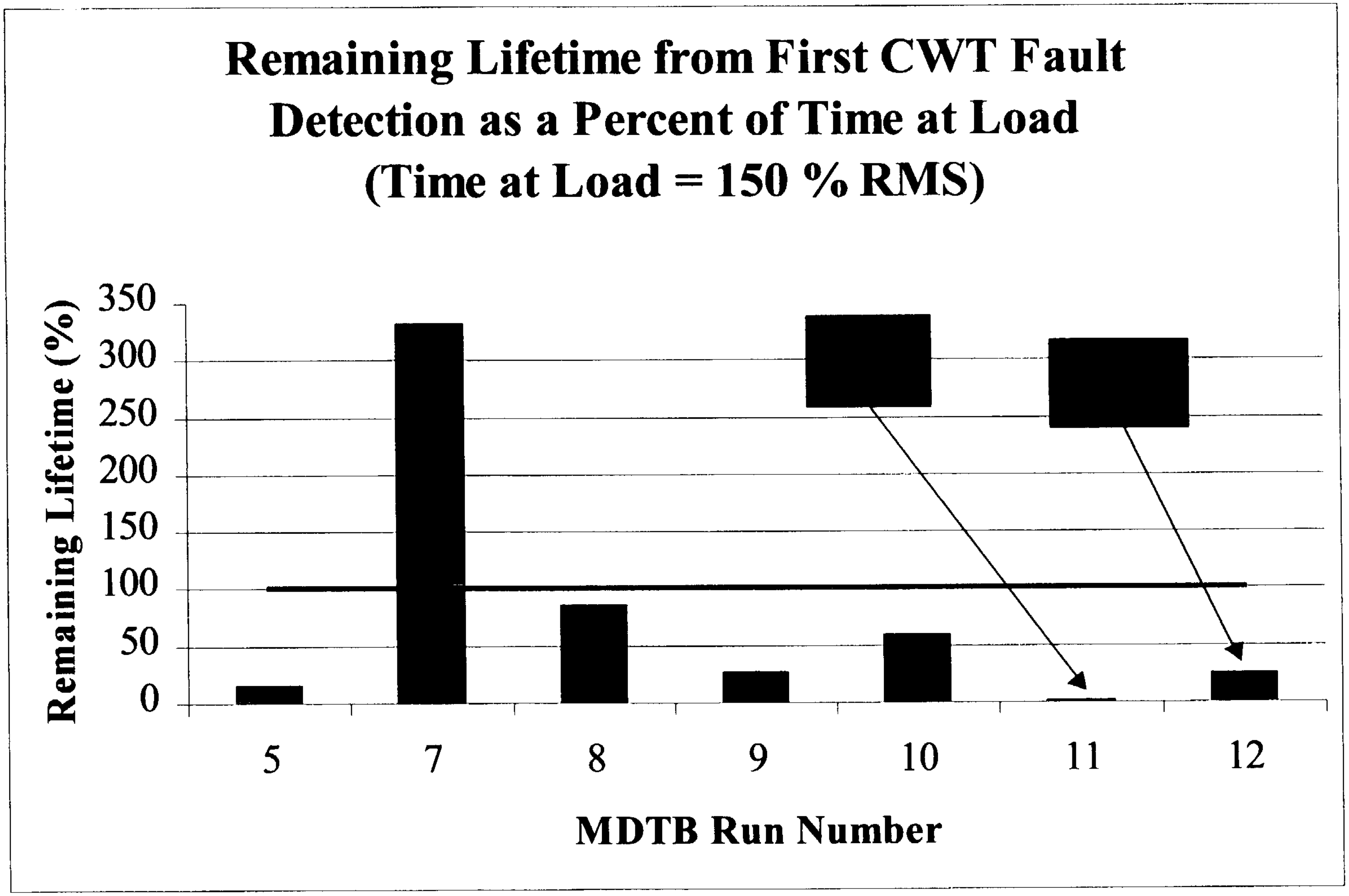

PENNSTATE

ARL

Wavelet Trigger

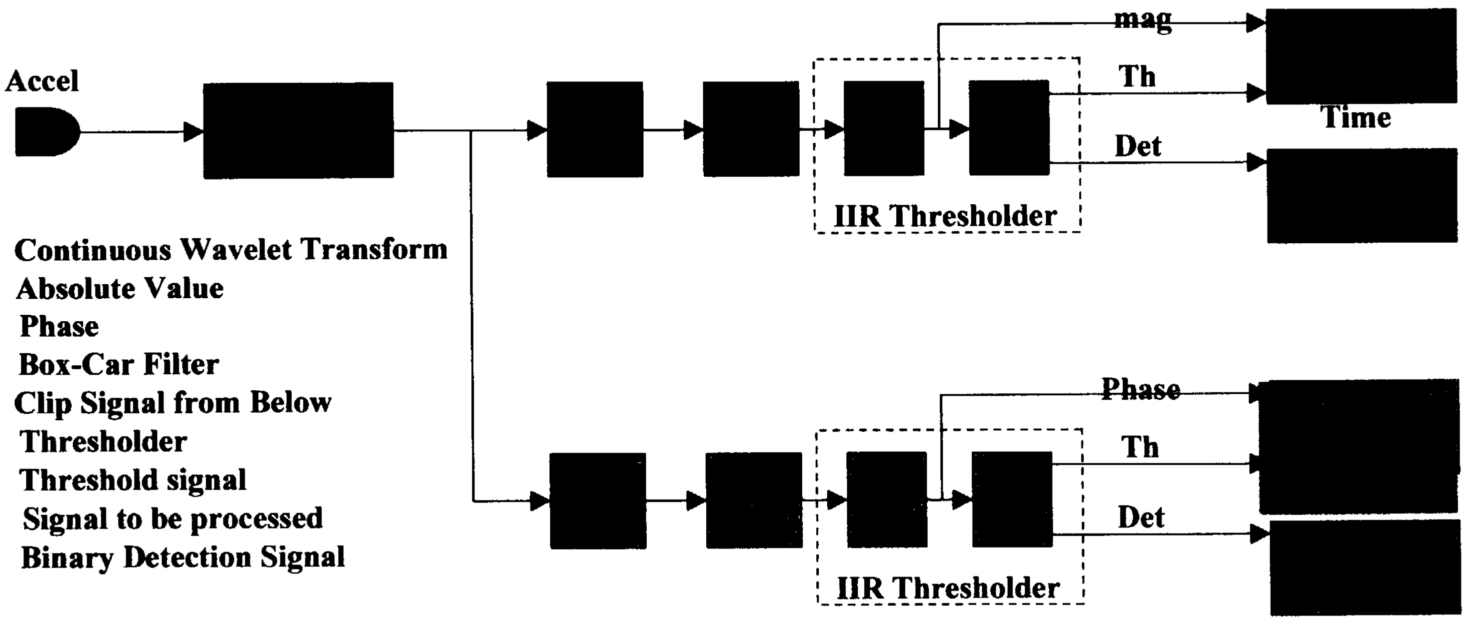

CWT:	Continuous Wavelet Transform
Abs:	Absolute Value
Ang:	Phase
B-C:	Box-Car Filter
Clip:	Clip Signal from Below
IIR:	Thresholder
Th:	Threshold signal
mag:	Signal to be processed
Det:	Binary Detection Signal

CWT Inputs:

- Number of Data Samples
- Sampling Frequency
- Number of frequencies
- Processing Frequencies

IIR Inputs:

P1 = 10	IIR filter Init. Value (dB)
FILB = 20	Clipping Level (dB)
N = 5	IIR filter memory (Integer)
Thold = 8	Detection Threshold (dB)
C1 = 1.95	IIR filter step response
C4 = -4	Track Threshold scale factor (dB)
flen = 3	Length of Box-Car filter
shif t= 2	Box-Car filter shift factor

PENNSTATE ARL

IIR Adaptive Threshold Tracker

- Robust at data level against F/As.
- Numerically efficient.
- **Question:** How do we set the IIR Threshold level to minimize F/As and maximize probability of fault detection?

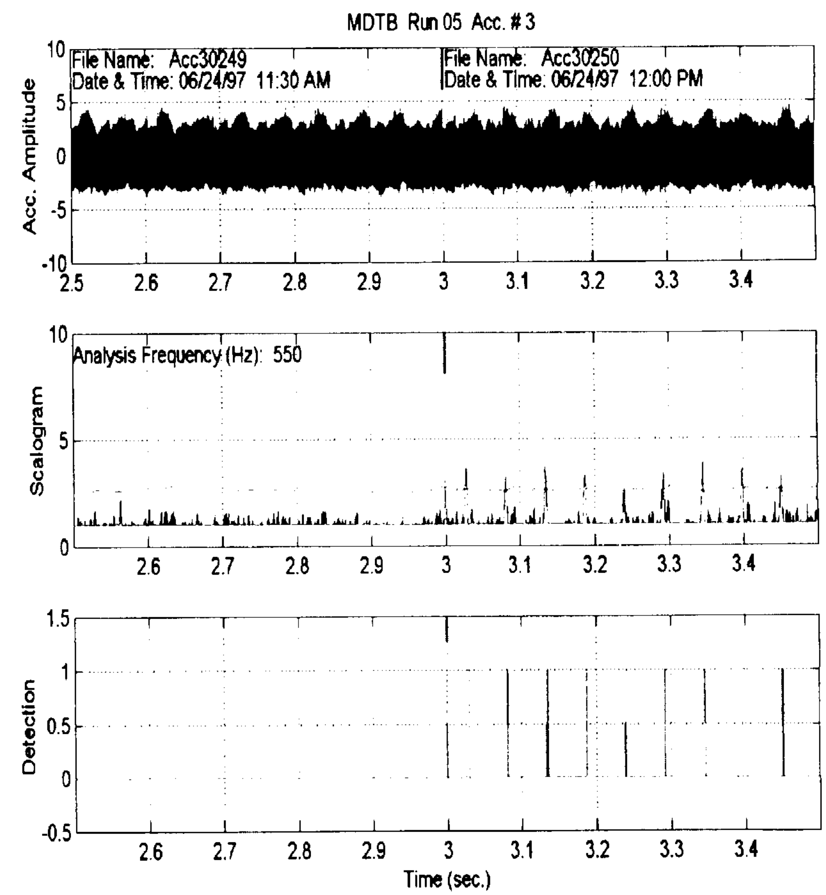

PENNSTATE ARL

The Statistical Characterization of Data

OBJECTIVES

- Establish general analytical procedures for setting alarm threshold levels associated with feature based (or FOM) fault detection algorithms used in machinery diagnostics.

APPROACH

- Apply the Goodness-of-Fit / Hypothesis Testing methods on the Continuous Wavelet Magnitude (squared) data of MDTB Run #5.
- Extend procedure to other runs and also to other detection statistics.

MDTB Testbed

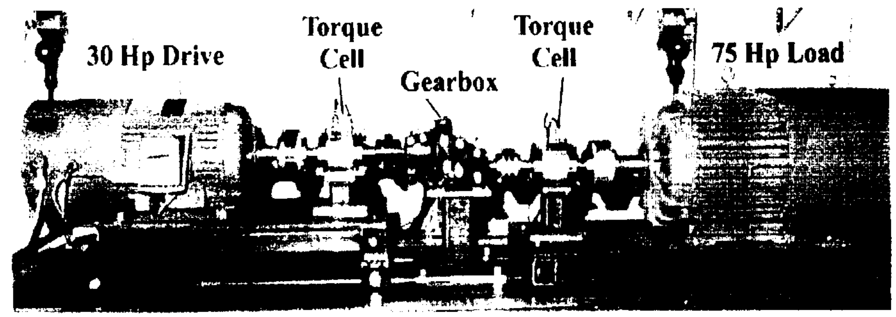

BENEFITS

- Provides a rigorous statistical method for ascertaining and selecting detection threshold settings for given false-alarm tolerances.

PENNSTATE

ARL

Goodness-of-Fit Methodology

- Define the random variable as the continuous (Morlet) wavelet magnitude (squared) computed at 550 Hz. [GM = 895Hz.]
- Goodness-of-Fit approach requires **stationarity** and independence of the data.
- Compute both the sample PDF and CDF of the data for fault and no-fault conditions at given operational speed & load.
- Select an appropriate family of distributions, e.g., Weibull, Exponential, Mixture, etc., in order to model the sample statistics:
  - can model statistic about mean
  - model statistic in L/R tail
  - physical basis of model

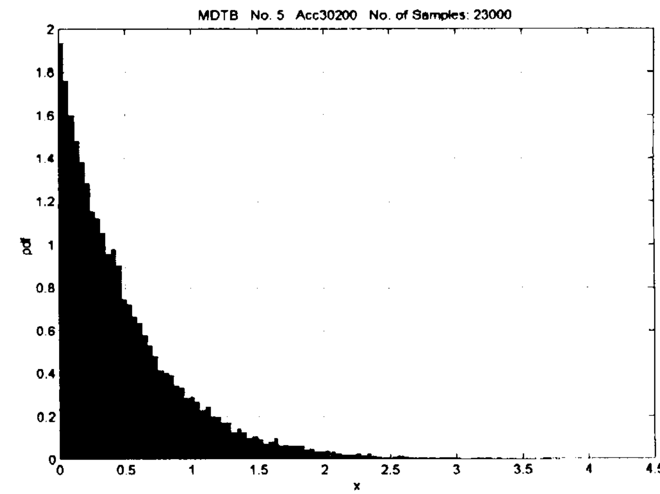

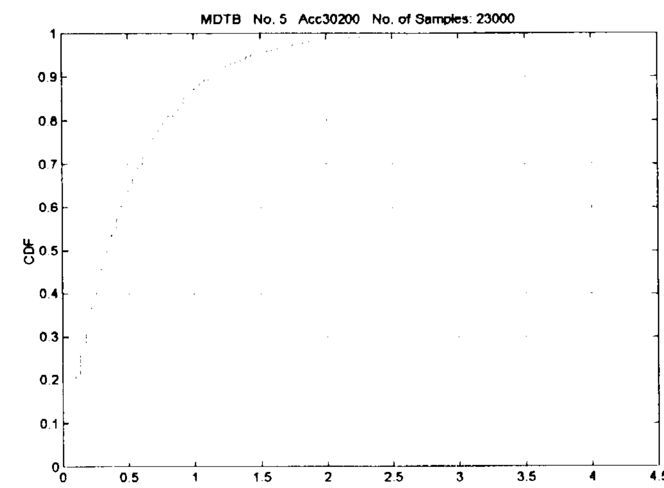

PENNSTATE ARL

Data Re-sampling (No-Fault Condition)

- To ensure data stationarity (3X loaded gearbox accel data)
  - Data files consist of 200,000 samples of CW -transformed data
  - Segment data in terms of shaft rotations (~ 1051 samples/rot)
  - Select a small number of samples (120 samp ~ 3 teeth from the same part of the rotation) for each rotation.
  - Merge / concatenate the samples from each rotation to form a representative no-fault sample data sequence for the 10-sec record cycle.

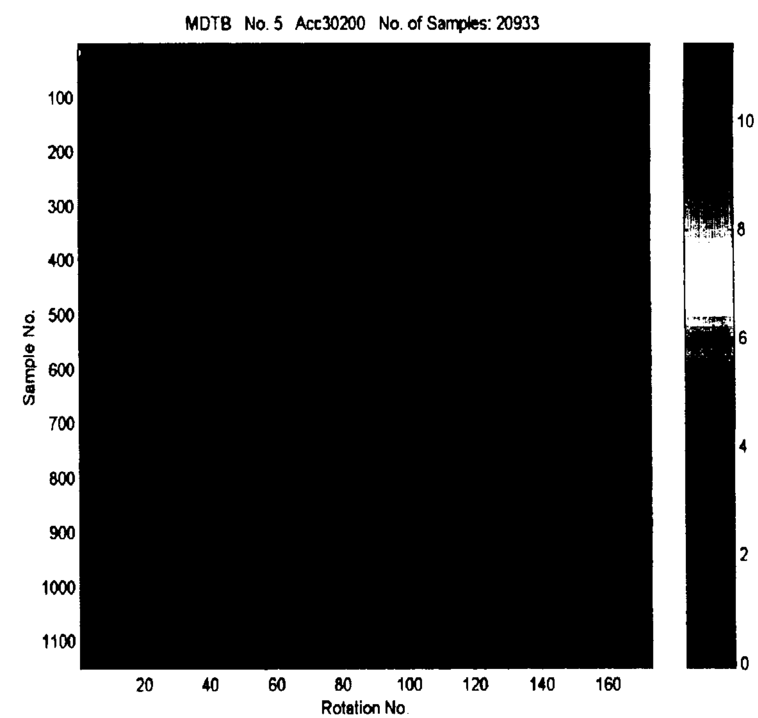

PENNSTATE ARL

(No-Fault) Data Correlation & Stationarity

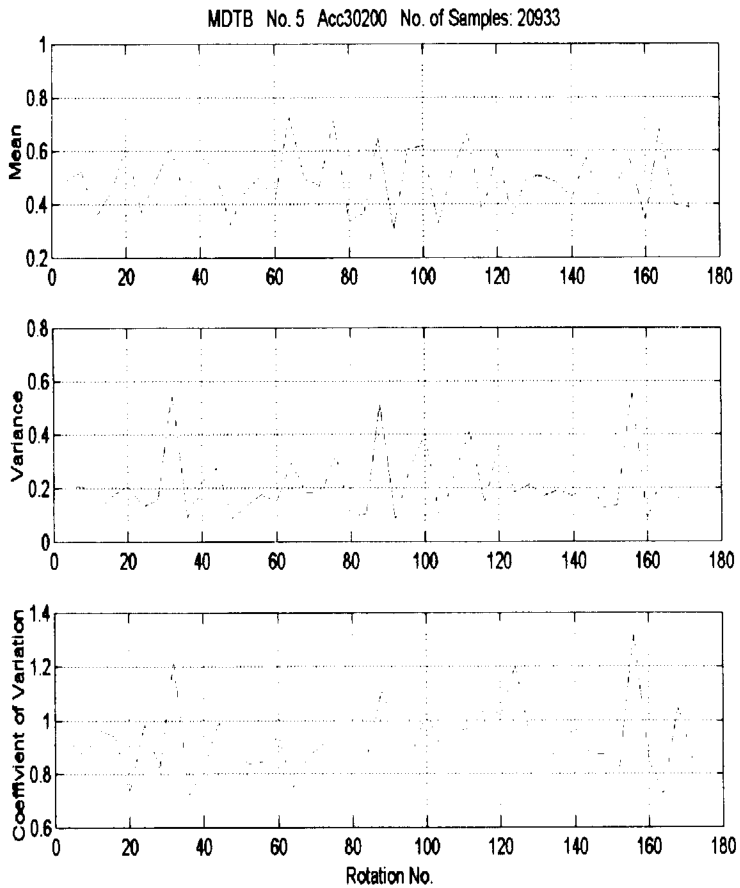

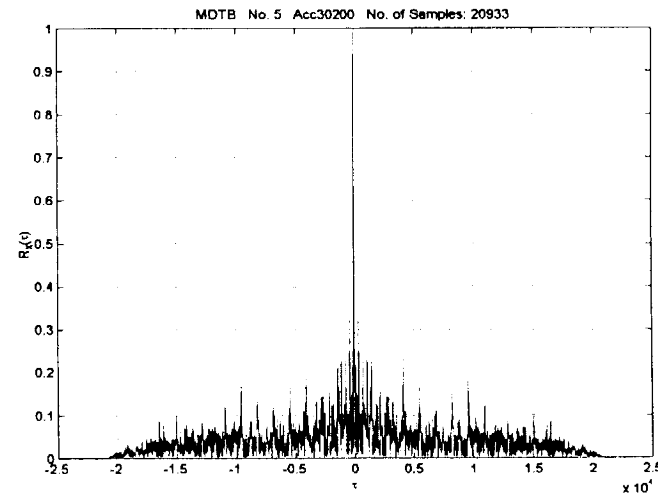

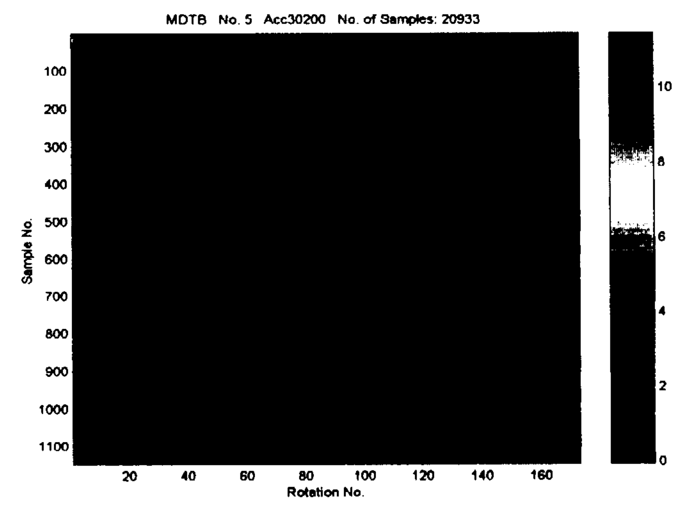

PENNSTATE 1855 ARL

Sample PDF / CDF
(3X Loading No-Fault Condition)

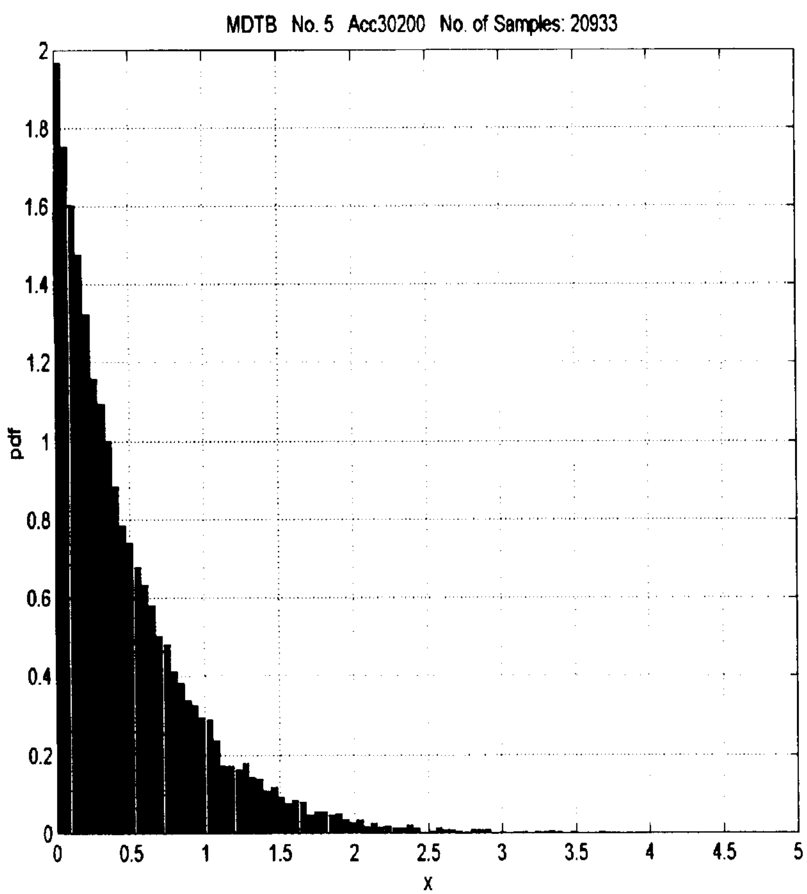

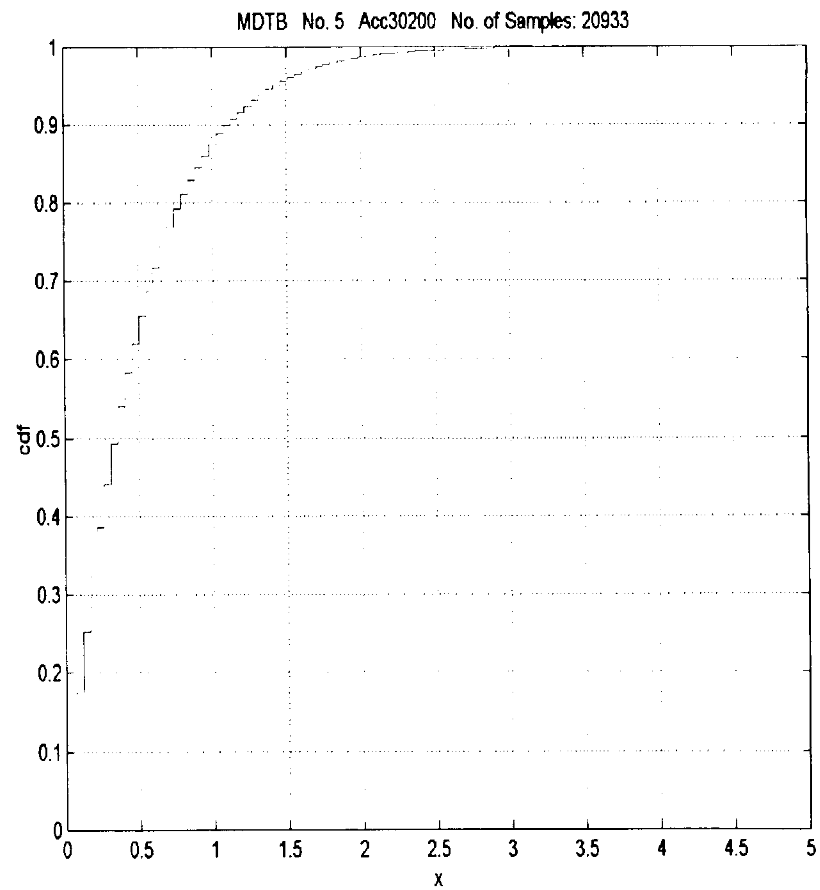

PENNSTATE ARL

Comparison of Sample PFA with Parametric Distributional Model (3X Loading No-Fault Condition)

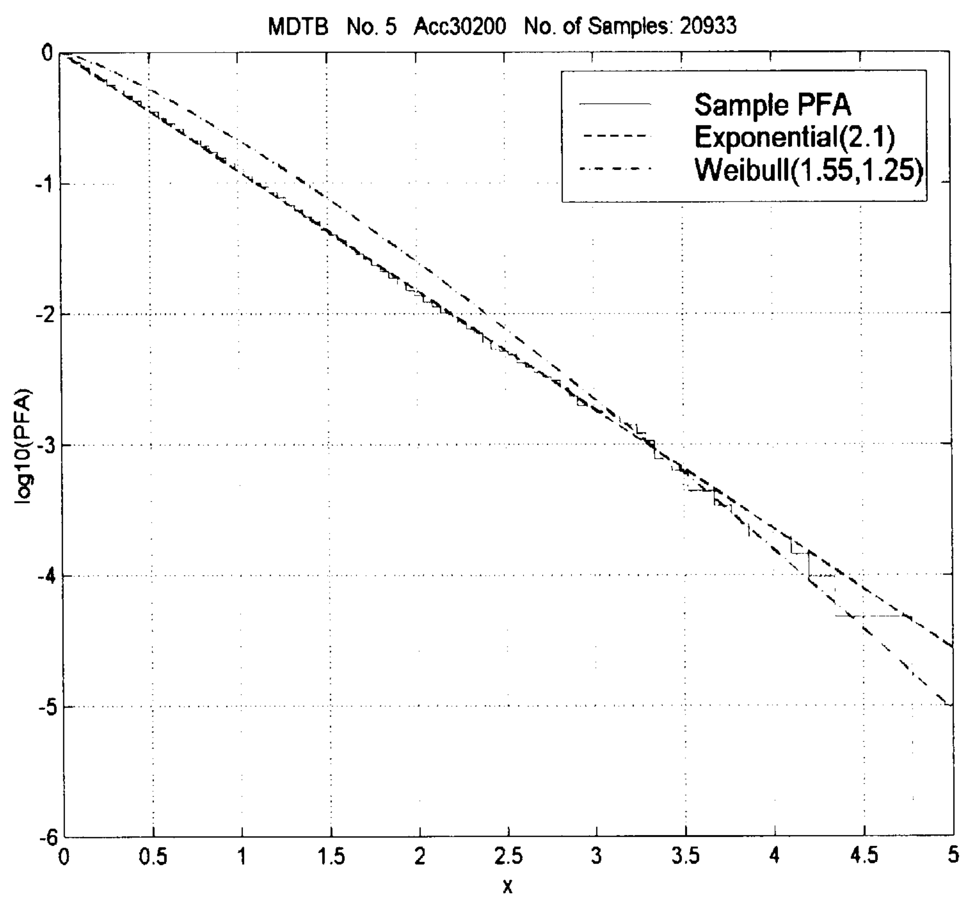

Comparison of Sample PDF / CDF with Parametric Distributional Model (3X Loading No-Fault Condition)

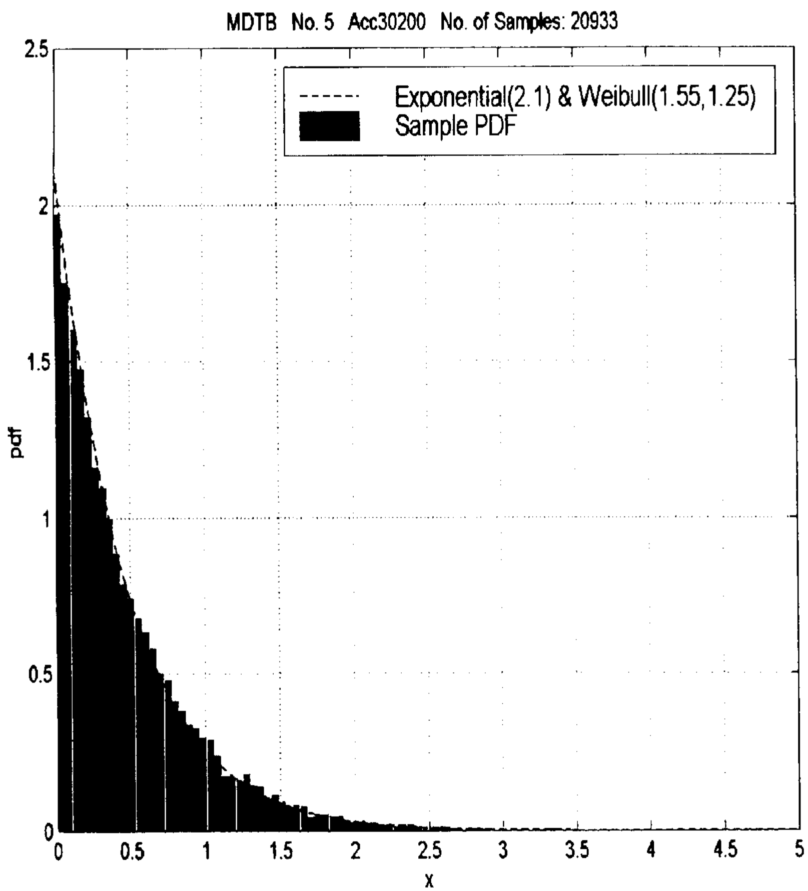

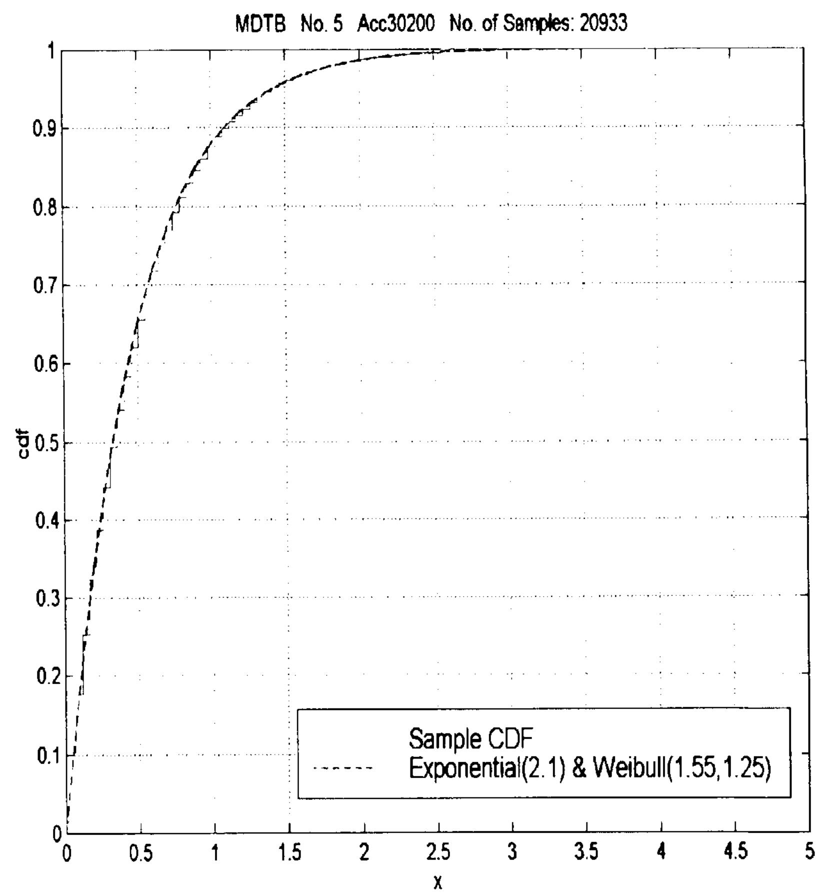

PENNSTATE ARL

Data Re-sampling (Fault Condition)

- To simplify the collection of signal-plus-noise data
  - Data files consist of 200,000 samples of CW -transformed data.
  - Select those samples which exceed a given threshold (see adjoining Figure).
  - These samples represent signal-plus-noise data sequence.

MDTB No. 5 Acc30250 No. of Samples 8087

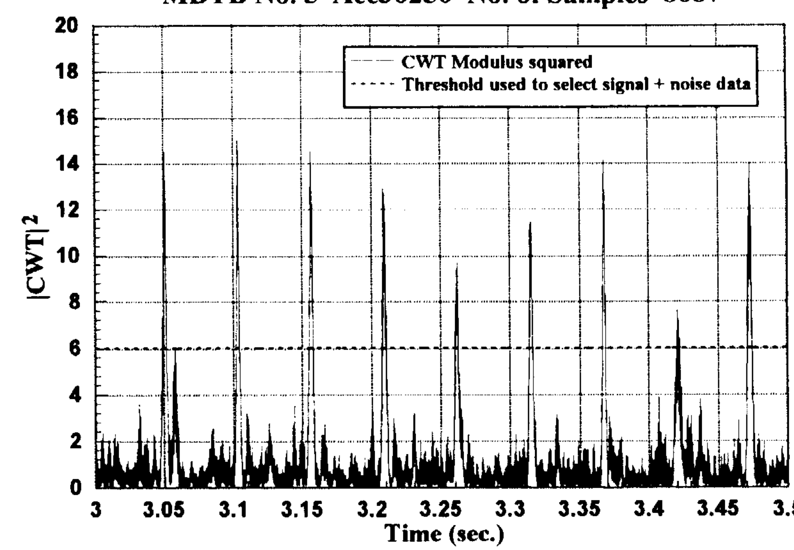

Sample PDF / CDF
(3X Loading Fault Condition)

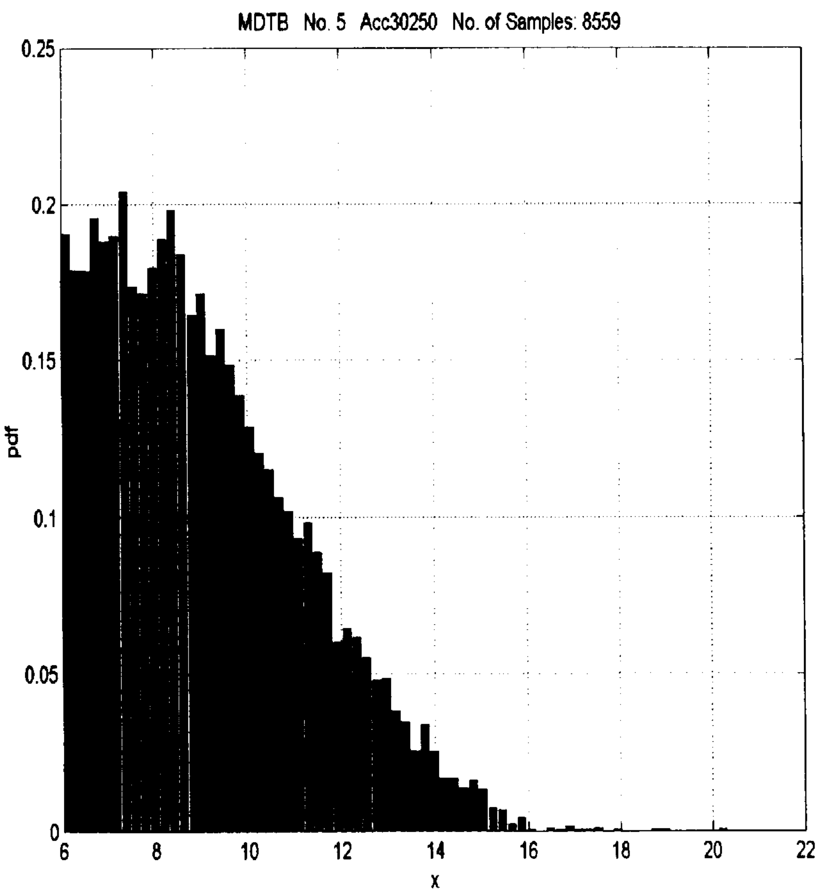

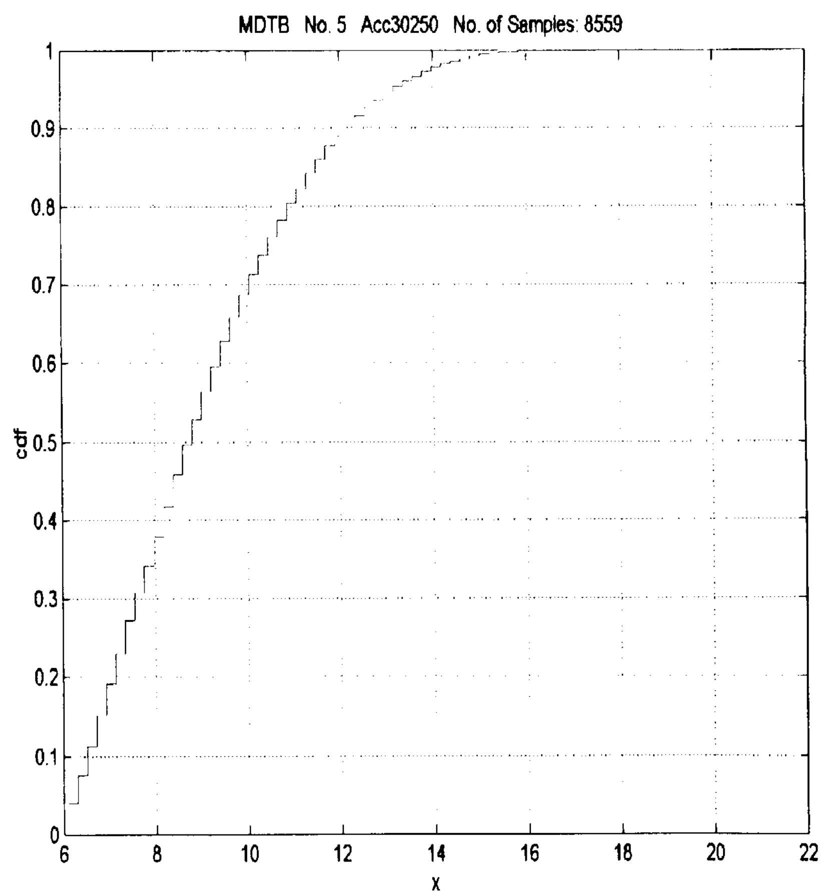

PENNSTATE ARL

Comparison of Sample PFA with Parametric Distributional Model (3X Loading Fault Condition)

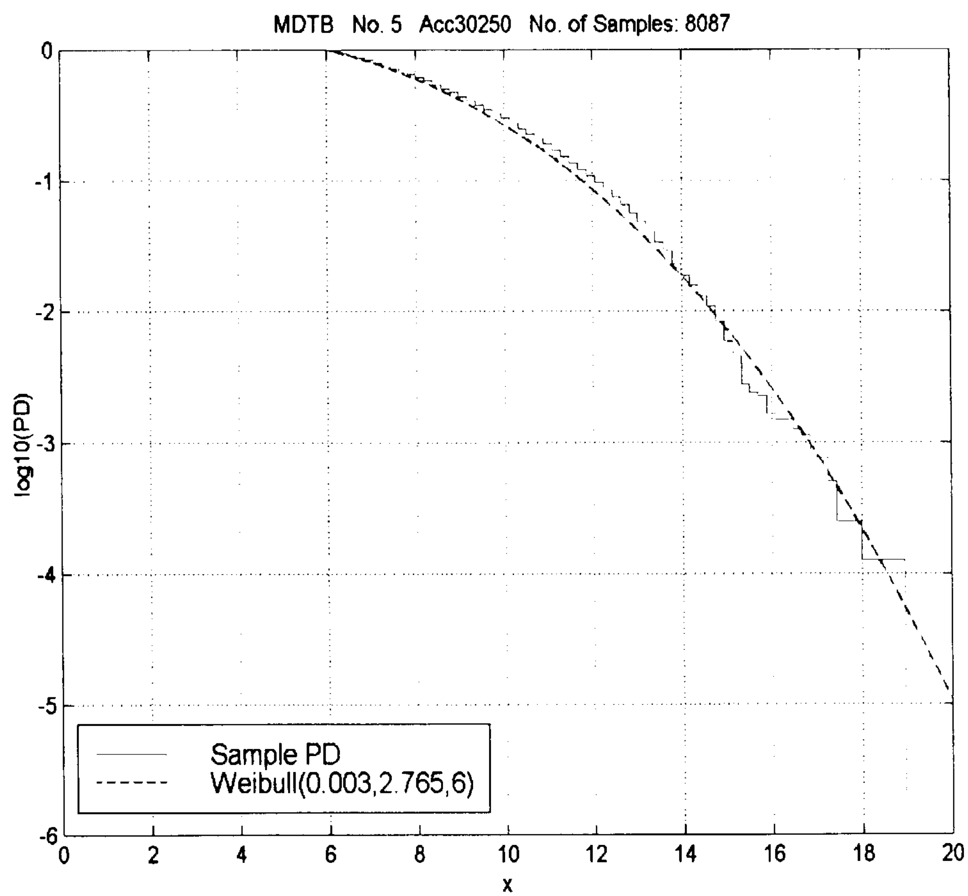

Comparison of Sample PDF / CDF with Parametric Distributional Model (3X Loading Fault Condition)

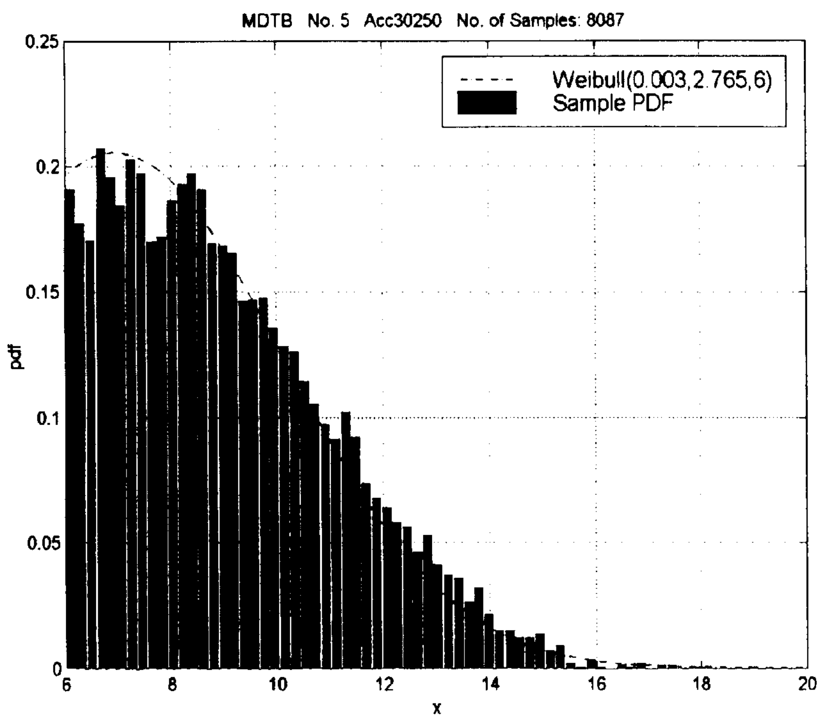

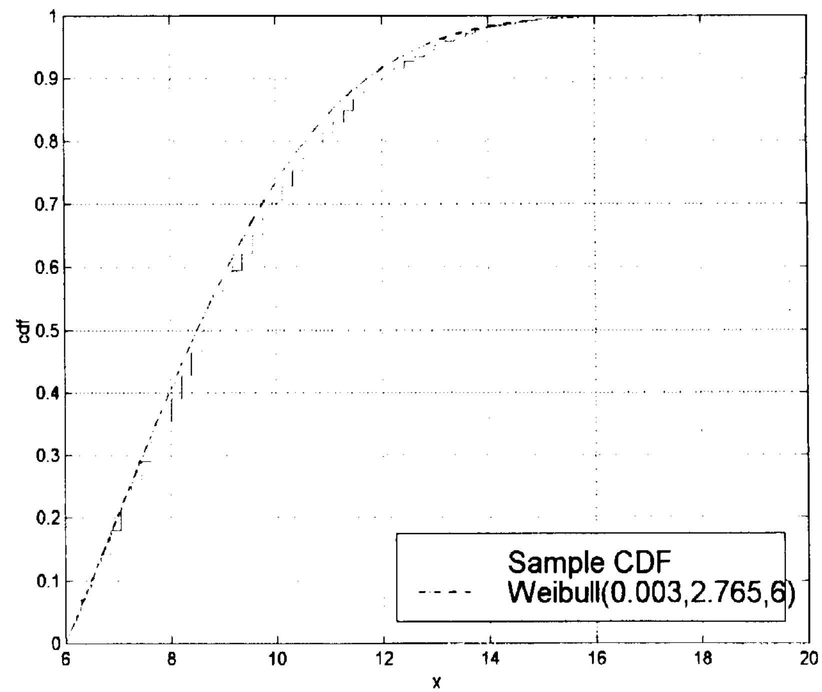

PENNSTATE ARL

Comparison of the Probability of False Alarm & Detection

- Run #5 Threshold level in [4,6] guarantees low F/As and high detection probabilities.
  - Perform additional analysis across multiple runs before hard conclusions can be reached
  - Identify the family of distributions and associated parameters which describes the wavelet magnitude (squared) coefficient for the MDTB / NASA gearbox feature data.
  - May entail mixture models for complete fit

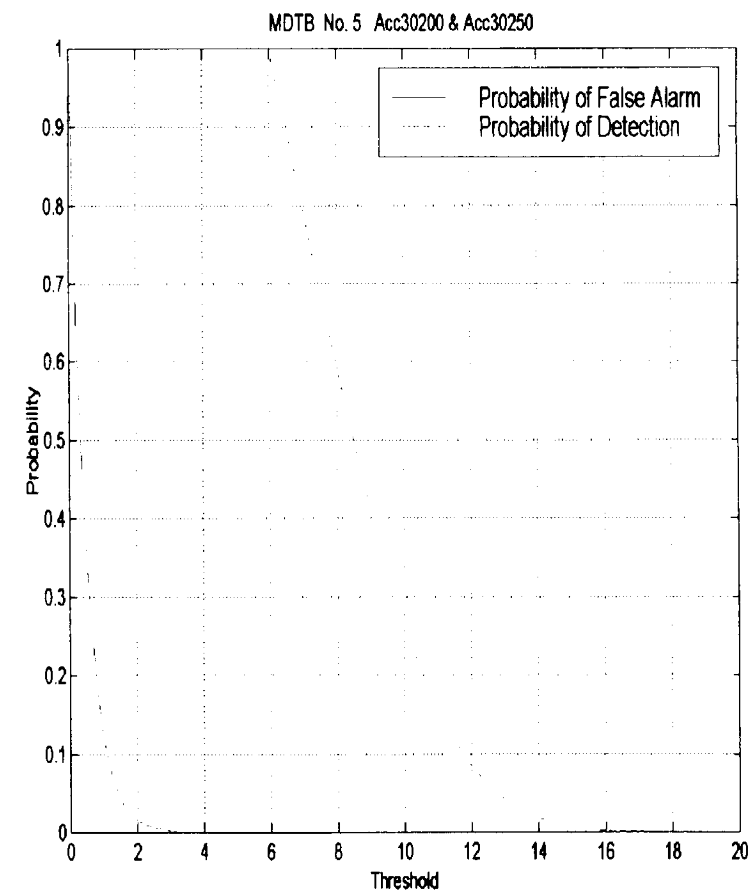

PENNSTATE

ARL

Future General SP Work

- Extend the statistical investigation to encompass other Figures of Merit (FOMs), e.g., FM4, NA4, enveloping, etc.
- Perform a comparative analysis of all the FOMs:
  - Earliest Detection (in-progress)
  - Best F/A performance
  - Most computationally efficient / easiest to automate
- Discrete Wavelet Transform on Acoustic Emission Data
  - counts / rate of change of counts
  - morphology of AE waveform
- Pass Wavelet data through (R)NN
- Image Processing / IR-based algorithms
- Delineation of effective gear / bearing / shaft / oil, temp, etc. sensor fusion Alg.

Fusion Toolkit
(Weighted Voting)

PENNSTATE

ARL

- MDTB Run #5: Non-commensurate sensor processing
- 4 Accelerometer Channels + 1 Temperature
- Data Input Formats:
    - MDTB
    - Ascii
    - Wav
- FTP Site: Oracle.arl.psu.edu (password protected)

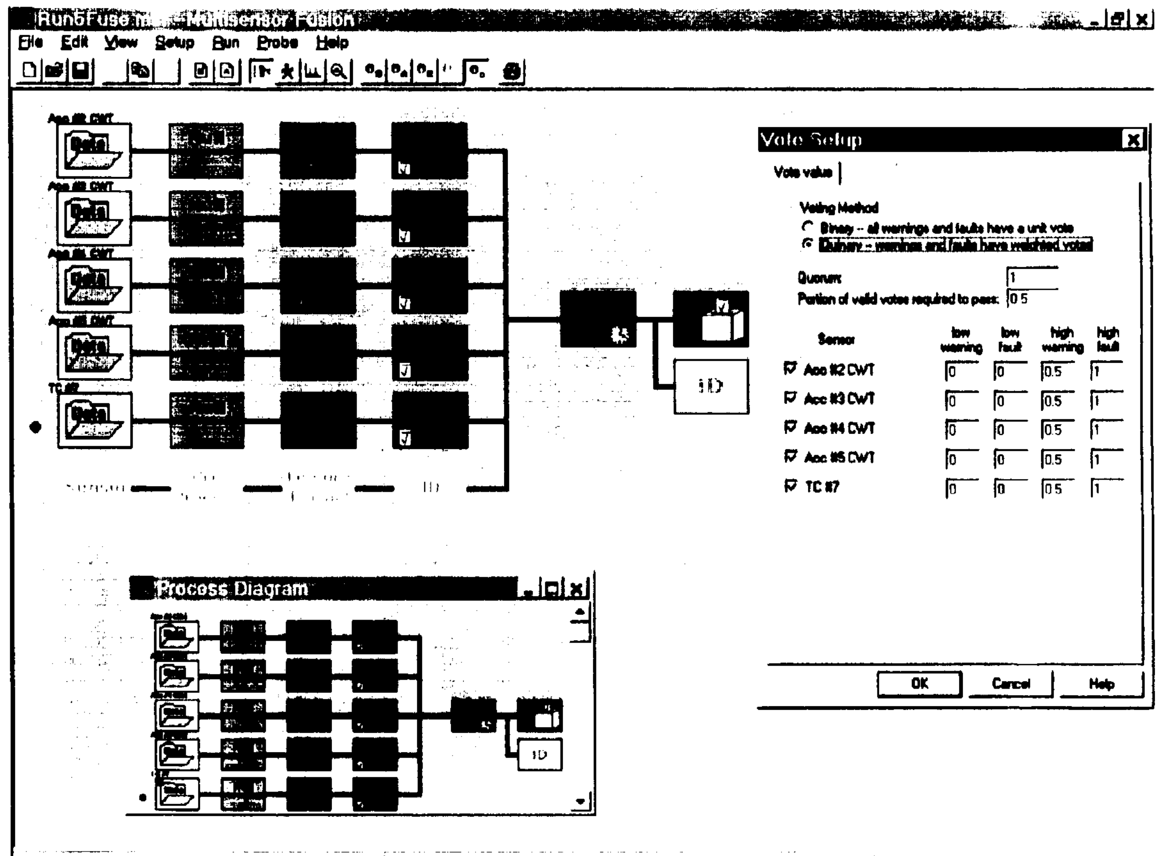

Fusion Toolkit
(Voting Results)

PENNSTATE ARL

- MDTB Run #5: Non-commensurate sensor processing
- 4 Accelerometer Channels + 1 Temperature
- 18 record cycles spaced 8 hours apart
- All 5 sensors are given equal weight: Threshold = 2.5

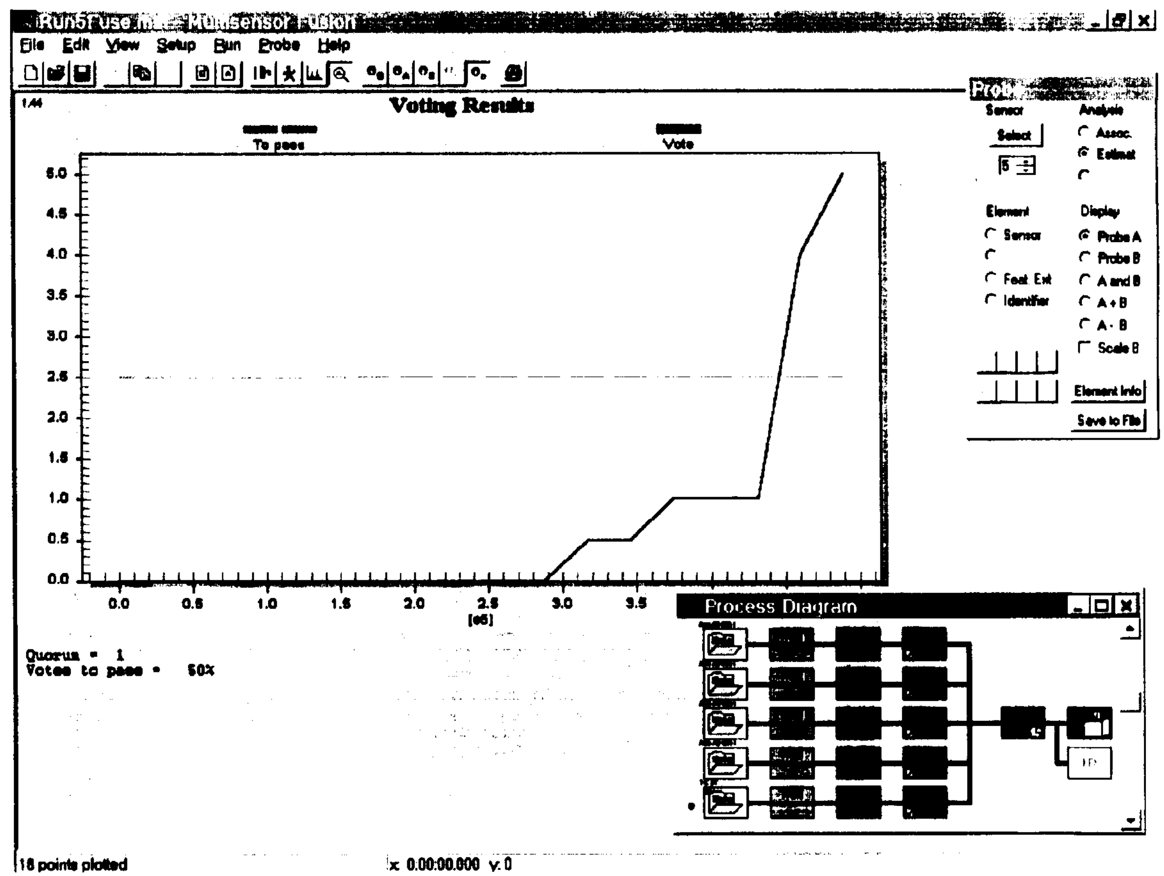

PENNSTATE

ARL

MS Fusion Toolkit

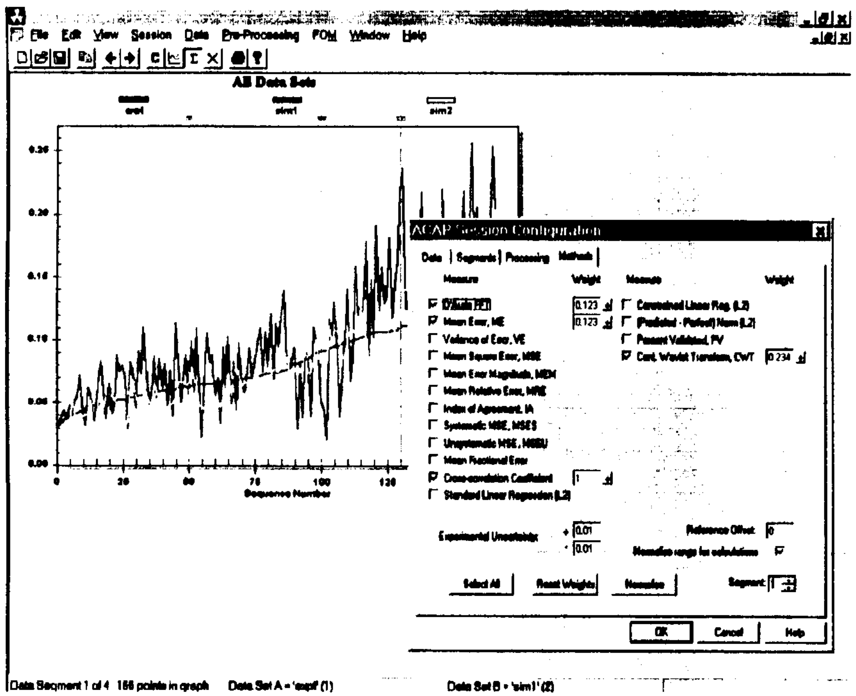

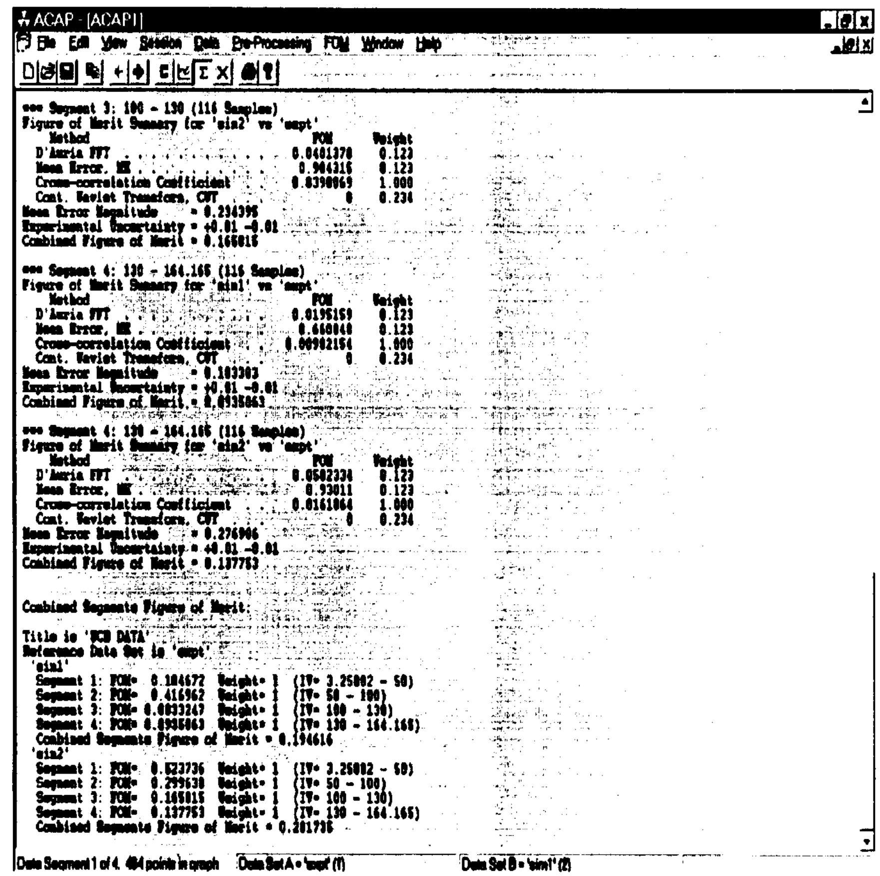

- Model Validation in different domains by way of comparison between simulated and operational field recorded data sets.

CINET
Fuzzy Logic Tool

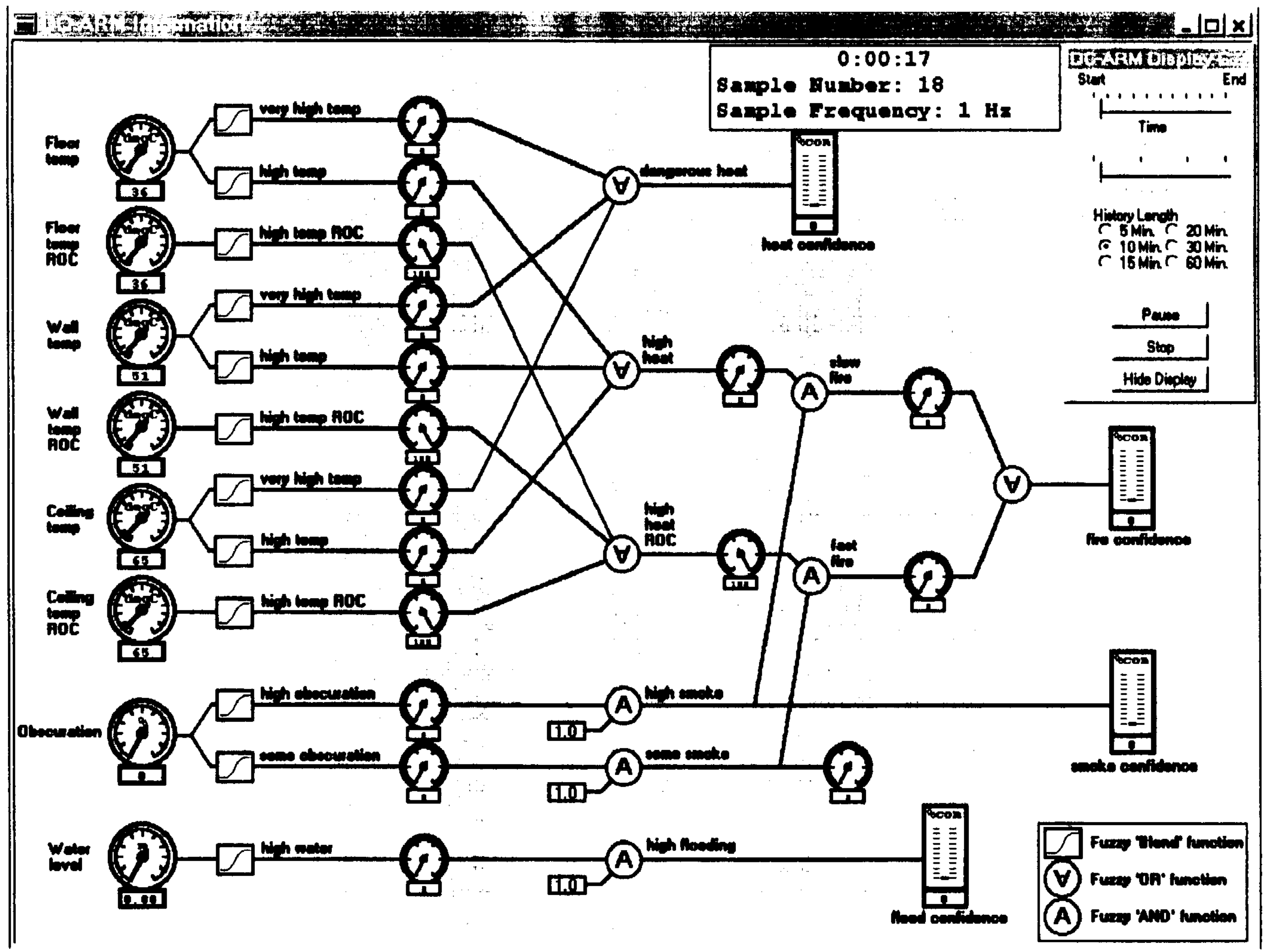

PENNSTATE ARL

MS Fusion Toolkit: Future Work

- Implement data block / segment averaging with specified overlap (e.g. chirp-z transform averaging)
- Additional Plug-ins / DLL modules, e.g., NNs.
- NASA Customization Features:
  - Batch processing set-ups using script files
  - By relaxing graphical interface feature, program can be ported to other platforms (e.g., LINUX, pipe to UNIX platforms)
  - Other

PENNSTATE

ARL

NASA Ames Research Center

12-Foot Pressure Wind Tunnel

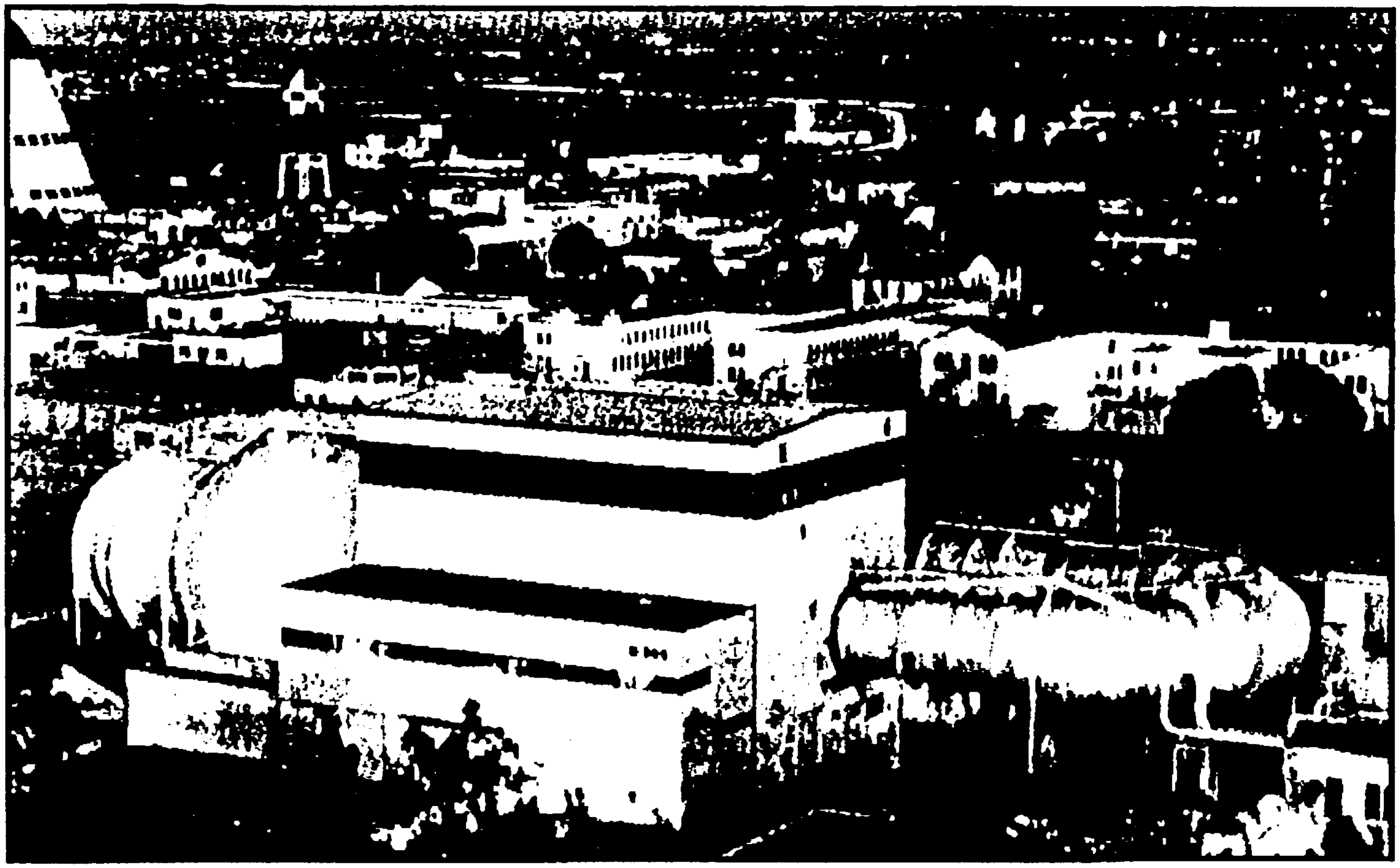

PENNSTATE ARL

Torsion

(K. Maynard)

PENNSTATE ARL

Future Tasking

	FML	12 Foot
Signal Processing & Statistical Analysis	♦ Data Trending: Run-up / SS / coast-down ♦ Proximity Probe data through the DAQ ♦ DWT on AE MDTB Data ♦ DF Toolkit – DLL Customization / Enhancements ♦ Threshold & FOM Statistical Characterization	♦ Quality Data Acquisition ♦ Data Trending: Run-up / SS / coast-down ♦ Threshold & FOM Statistical Characterization
Automated Reasoning	♦ Develop Expert System / Fuzzy Logic Diagnostic Rules ♦ Develop Hybrid NN Diagnostic System ♦ Investigate NN Prediction with Wavelet Data	♦ Develop Expert System / Fuzzy Logic Diagnostic Rules ♦ Develop Hybrid NN Diagnostic System
Modeling	♦ Hydrodynamic Fluid-film Bearing Models ♦ ANSYS Modeling of MDTB / FML GBs ♦ NN Model Approximation ♦ TSU Bearing Diagnostic Methods	♦ Medium Fidelity Model of Sub-systems ♦ TSU Bearing Diagnostic and fault simulation methods

ABSTRACT

Condition-Based Maintenance (CBM) requires the identification and tracking of the sensor observables capable of indicating faults and the ability to relate these variables to the overall health and remaining useful life of the machine. The progress on developing suitable dynamic models for diagnosing and tracking mechanical systems failure is reviewed. The objectives are to provide physical understanding and context to the association between damage severity and observables and support future implementation of data fusion and model-based prediction methods. The developed methodology is applicable to both the MURI IPD Program and NASA Ames driveline diagnostics. An overview and technical results are provided.

NASA Ames Research Center under Subcontract GFY900240 and the Office of Naval Research under ONR Grant: N00014-95-1-0461 has provided support for this work. The report was compiled with input from additional ARL personnel, Ken Maynard, Terri Merdes, and Colin Begg.

TABLE OF CONTENTS

LIST OF FIGURES

1. INTRODUCTION

This work was performed under sponsorship of the NASA Ames Research Center and the Office of Naval Research to improve the methodology in model-based prediction of machinery faults. The modeling thrust is focused on the development of methods using explicit non-linear diagnostic and prognostic models for mechanical systems failure. The thrust is coordinated with the sensor techniques to provide association between damage severity and observables, and it supports the implementation of data fusion and reasoning based upon model-based prediction methods.

The development of model-based prognostic capability for CBM requires a proven methodology to create and validate physical models that capture the systems' dynamic response under normal and faulted conditions. In heavy duty and high-performance power transmission systems, the rotary elements can be driven to catastrophic failure through many types of mechanisms. Subsystem component defective material and even normal wear can lead to fatigue stress cracks. Damage initiated by transient load swings due to larger magnitudes and higher than expected amounts of intermittent loading cycles can also occur in a system when operational performance limits are chronically commanded. For a majority of systems, operational demands prescribe a slow (as compared to operational speed or the length of a given machine service event) evolution in material property and/or component apparent configuration changes. The potential thus exists to track the fault through the (filter of the) system's behavior via it's dynamic (vibratory) response.

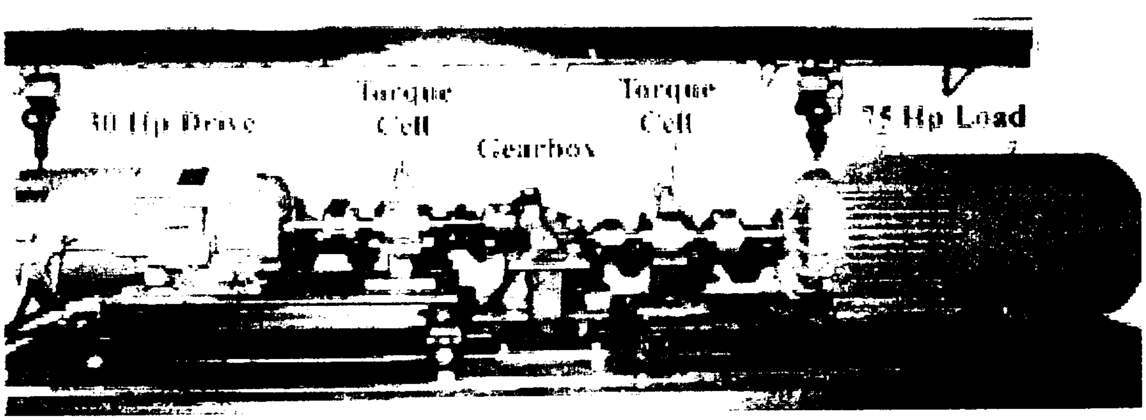

Figure 1. ARL Mechanical Diagnostics Test Bed is a key facility for developing transitional failure data sets and developing prediction methodology

Statically, and in terms of life cycle fatigue behavior, faults and failures in gear pairs, rotary shafting, and bearings is fairly well understood but dynamic response and tribological information is lacking for machines operating to failure. This shortcoming is precisely the motivation behind the development of the Mechanical Diagnostics Test Bed (MDTB), which was developed by ARL to provide transitional failure data on gearboxes and is shown in Figure 1.

Specific computational results and experimental validation methods based on a thorough review of the state of the art in drive system modeling are presented. A methodology for modeling the gearbox system under normal and faulted conditions is presented in the context of developing a model-based prognostic approach.

2. SUMMARY OF TECHNICAL PROGRESS

Task	Performers	Objective	Task Description
Dynamic Mechanical Systems Models	Ken Maynard Colin Begg Terri Merdes Carl Byington	Develop mechanical systems and fault models for predicting MDTB failures.	1. Torsional response and mode shape ANSYS model 2. System-level multi-DoF dynamic ANSYS models 3. Subsystem-level, multi-DoF gearbox models 4. Fault injection/assoc. methods
Experimental Characterization	Colin Begg Jeff Banks Jim Kozlowski	Characterize the MDTB structural response and gearbox dynamics for model validation.	1. MDTB driveline frequency response function estimation 2. Subsystem modal analysis 3. Computer model validation

3. MODELING APPROACH

The mechanical systems modeling effort is comprised of computational and experimental work to understand, model, and correctly predict the evolution of faults in the MDTB system. The gearbox system model serves as a numerical study test bed to aid in optimal, or development of a best, sensor location strategy for CBM. Computational modeling efforts include the definition of finite element modeling and experimental identification/characterization of system modal and transfer characteristics. Analytical dynamics models of gear mesh, rotating shaft, and bearing faults will be adapted for integration and inclusion into an overall system model as nonlinear system perturbation forces.

4. CURRENT RESEARCH RESULTS

At the Pennsylvania State University (PSU) a Mechanical Diagnostics Test Bed (MDTB), Figure 1, of a geared mechanical rotor power transmission system has been designed and built. In the past, rotor system test beds have been constructed [Badgley et. al., 1974] to aid in the development of improved analysis and design capabilities of overall system rotor drive performance. The MDTB was designed specifically for the generation of transitional data to aid in the development of fault signature recognition and tracking algorithms [Byington et. al., 1997]. The MDTB is comprised of nine components that contain rotating elements. They consist of a variable speed AC drive motor, (2) tachometer/torque sensors (one for gearbox input and one for output), a single stage reduction helical gearbox, a load generator, and (4) shaft couplings ((3) gear and (1) chain type). An accompanying constant speed variable torque control system can be used to produce any form of normal to overload duty cycles required for long duration testing. The system is equipped with a data acquisition system that can provide numerous channels of continuous long duration records for any combination of accelerometer, torque, speed, and thermocouple sensor measurement signals. Faults that have been generated and studied to date, consist of overload generated gear tooth root cracks and gearbox cracked rotor shafts.

Many researchers and engineers have thoroughly investigated individual components and systems where a few critical components are coupled together in rotor power generation and transmission machinery. Many notable contributions have been made in the analysis and design, and in increasing the performance of rotor systems, and in the fundamental understanding of different aspects of rotor system dynamics [Dimentberg, 1961; Todl, 1965; Dimarogonas, 1983; Rao, 1983; Vance, 1988; Childs, 1993; Kramer, 1993; Lee, 1993; Dudley, 1994; LaLanne et al., 1998]. More recently, for ergonomic as well as design reasons, many commercial and defense efforts have been focused on the prediction of vibration and noise from gearboxes in power transmission [Mitchell et al., 1982; Ozguven, 1988; Choi et al., 1990; Lim et al., 1991; Kahraman, 1993]. With the recent interest in system health monitoring [Rao, 1996] the modeling of complete geared power transmission rotor systems with faults has arisen. The motivation to develop a system model comes from the need to have time history response data from system monitoring sensors available for signal processing and fault detection algorithm development and testing. A computational model could allow immediate feedback on algorithm performance, and mitigate time consuming and costly testing. Additionally a model could be used to better ascertain the best specifications for, and placement of measurement sensors, and provide a means for efficient evaluation of fault extraction models used in fault signature recognition algorithms.

4.1. DYNAMIC MECHANICAL SYSTEMS MODELING

The overall objective of the MDTB modeling effort is to obtain a system model that can be used for system dynamics analysis and simulation. Simulation is required to provide time history responses of vibratory states (displacements, velocities, and accelerations) at desired sensor locations in and around the system gearbox. States generated by typical, multiple, rotor system sources of excitation - rotor disk unbalance, coupling misalignment, gear mesh mechanics, and roller bearing dynamics are of prime interest, see Equation 1 and Figure 2.

To achieve the modeling objective an approximate nominal linear lumped parameter characterization of the system is necessary. For the system gearbox model, disturbances are considered as time varying parametric excitations and N per revolution (N being an integer) periodic forces. Models of specific gearbox faults – gear tooth root fracture [Randall, 1982; McFadden et al., 1986] rotor shaft fracture [Nelson et al., 1986; Wauer, 1990; Wauer, 1990; Jun et al., 1992], and bearing wear defects [Dyer et al., 1978; Braun et al, 1979; McFadden et al., 1984] provide relevant fault modeling background. System faults are emulated via the integration of perturbations into the system excitations and forcing. System modeling expectations will be met if the model-generated vibratory states can be used to imitate signature changes in response to fault perturbations. As is typical during condition monitoring circumstances, constant speed and torque operating conditions will only be considered for models synthesized of the overall system.

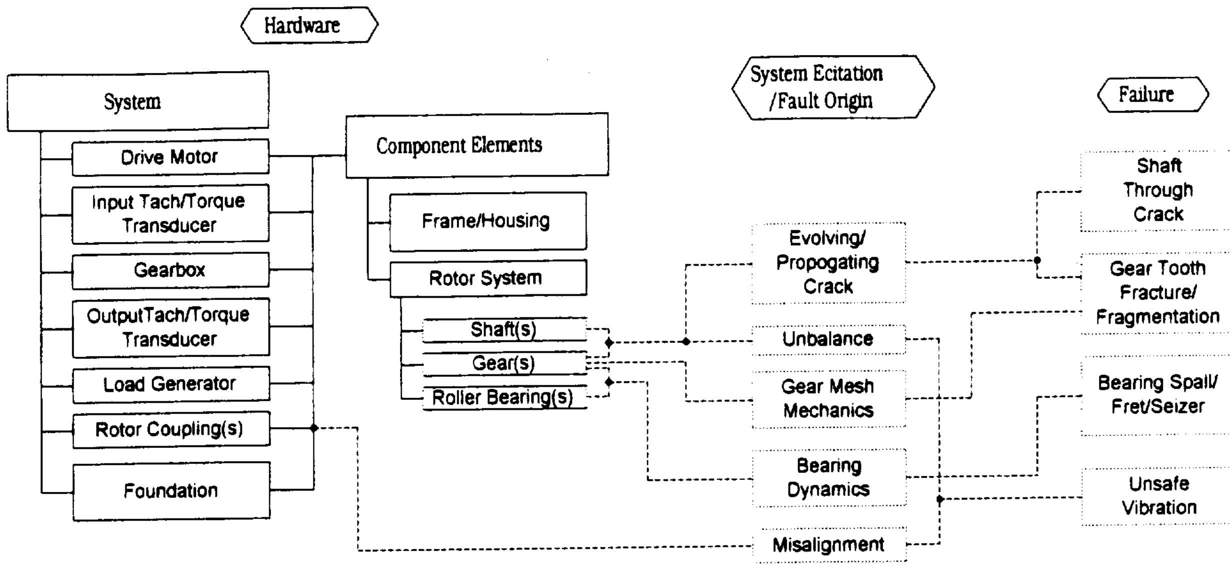

Figure 2. System Modeling Approach and Fault Introduction

$$\{M\}\ddot{\bar{y}}+\{C+G\}\dot{\bar{y}}+\{K+\Delta K_{fault}(t)+\delta\Delta K_{fault}(t)\}\bar{y}=\bar{F}(t)-\delta\bar{F}_{fault}(t) \qquad (1)$$

FEM is used to assemble the approximate nominal linear system mass, gyroscopic, and stiffness, matrices, {M}, {G}, and {K}, and an estimate of the linear system viscous damping, {C}, is produced from experimental modal analysis. Changes in forcing function and effective stiffness values are represented by the equation.

4.1.1. Torsional Structural Response Model

The Condition-Based Maintenance (CBM) Department at the Pennsylvania State University Applied Research Laboratory developed a transitional modal analysis modeling process, using ANSYS to model the Mechanical Diagnostic Test Bed (MDTB). ANSYS [Swanson Analysis Systems, 1994] is a modeling software package for finite element analysis and design, which can be used in many disciplines of engineering–structural, mechanical, electrical, electromagnetic, electronic, thermal, fluid and biomedical.

The procedure of solving a system of simultaneous differential equations of motion by transforming them into a set of independent equations by means of the modal matrix (associated with mass and stiffness matrices) is referred to as *modal analysis*. In this method the expansion theorem is used, and the displacements of the masses are expressed as a linear combination of the normal modes of the system. This linear transformation uncouples the equations of motion so that we obtain a set of n single degree of freedom systems, can be readily obtained. Modal analysis helps in understanding vibrational characteristics by calculating the natural frequencies and mode shapes of a linear system, which are important parameters under dynamic loading conditions.

The system, shown in Figure 3, composed of shafts, couplers and rotors. These are each modeled as elastic straight solid pipe with linear through thickness (ANSYS structural mass element "*pipe16*"). Both the 30 Hp and 75 Hp torque cells are modeled using point loaded mass elements ("*mass21*"). The gear mesh stiffness of the gearbox is represented as a ("*combination14*") element allowing for torsional capability; this is a purely rotational element with three degrees of freedom at each node, with no bending or axial load considerations. Once this model was constructed and the loads were applied with the appropriate degrees of freedom, the model was run to validate the densities and explore the effects of varying the spring constant.

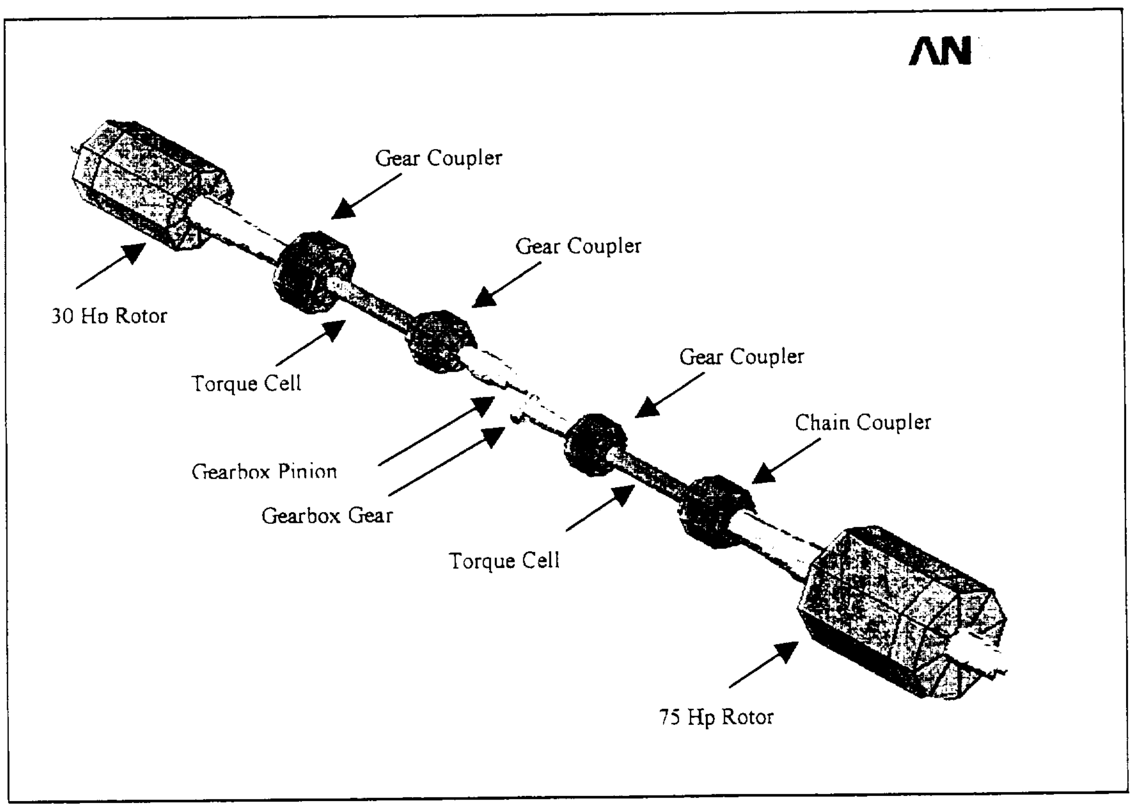

Figure 3. ANSYS torsional models of MDTB provides mode shape and dynamic response prediction

The gear mesh stiffness is a significant variable in the estimation of dynamic characteristics of the driveline. The stiffness constants for mesh deflection of the teeth are difficult to estimate with certainty. Some tests to determine this parameter are reported in technical literature, but the data is still rather limited due to the fact that the gear teeth are very stiff. Load distribution is one of the most complex subjects in gear design for the following reasons.

- Helical spiral of pinion does not typically match helical spiral of mating gear resulting in a (helix error effect).
- The pinion body bends and twist under load so that there is a mismatch between pinion and the gear teeth resulting in (deflection effects)
- Centrifugal forces distort the shape of the pinion or gear and mismatch the teeth, (centrifugal effects).

Deliberate design modifications, such as crowning, easement, or helix correction, concentrate the load in one area and relieve the load in another area. This is usually done to lessen the effect of one of the preceding items, but it is an effect in itself (design effects).

Darle W. Dudley found through tests on gear teeth, that a good average value for a typical gear design was a gear mesh stiffness constant of 2,900,000 psi to be used as a multiplier on the face width (F) measured in inches and the radius squared (Equation 2). Using this equation, with the MDTB gear data, the fundamental torsional mode frequencies are predicted in Figure 4.

$$K_{\theta}=(r)^2(2{,}900{,}000\ \text{lb/in}^2)(F) \qquad [\text{lb-in}] \qquad (2)$$

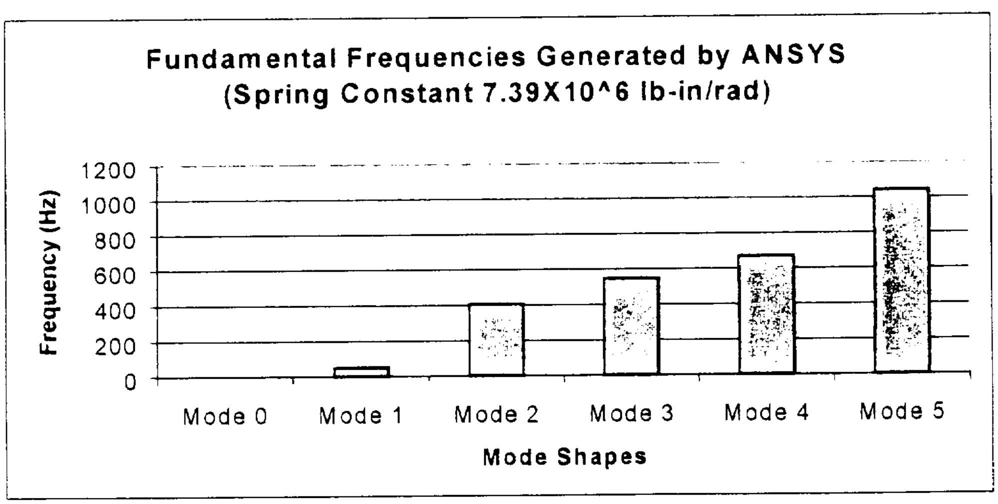

Figure 4. Fundamental mode shape frequencies predicted by ANSYS model using Dudley's equation

The gear mesh stiffness represented by a spring constant was changed by several orders of magnitude, to determine the sensitivity of this unknown on the fundamental frequency values. When the spring constant increases above the nominal value, there is very little effect on the natural frequencies; however, the natural frequency showed a marked sensitivity to the spring constant when they are decreased below the nominal value, as shown in Figure 5. Quantification of this effect is necessary to fully validate the model and understand the structural behavior of the MDTB.

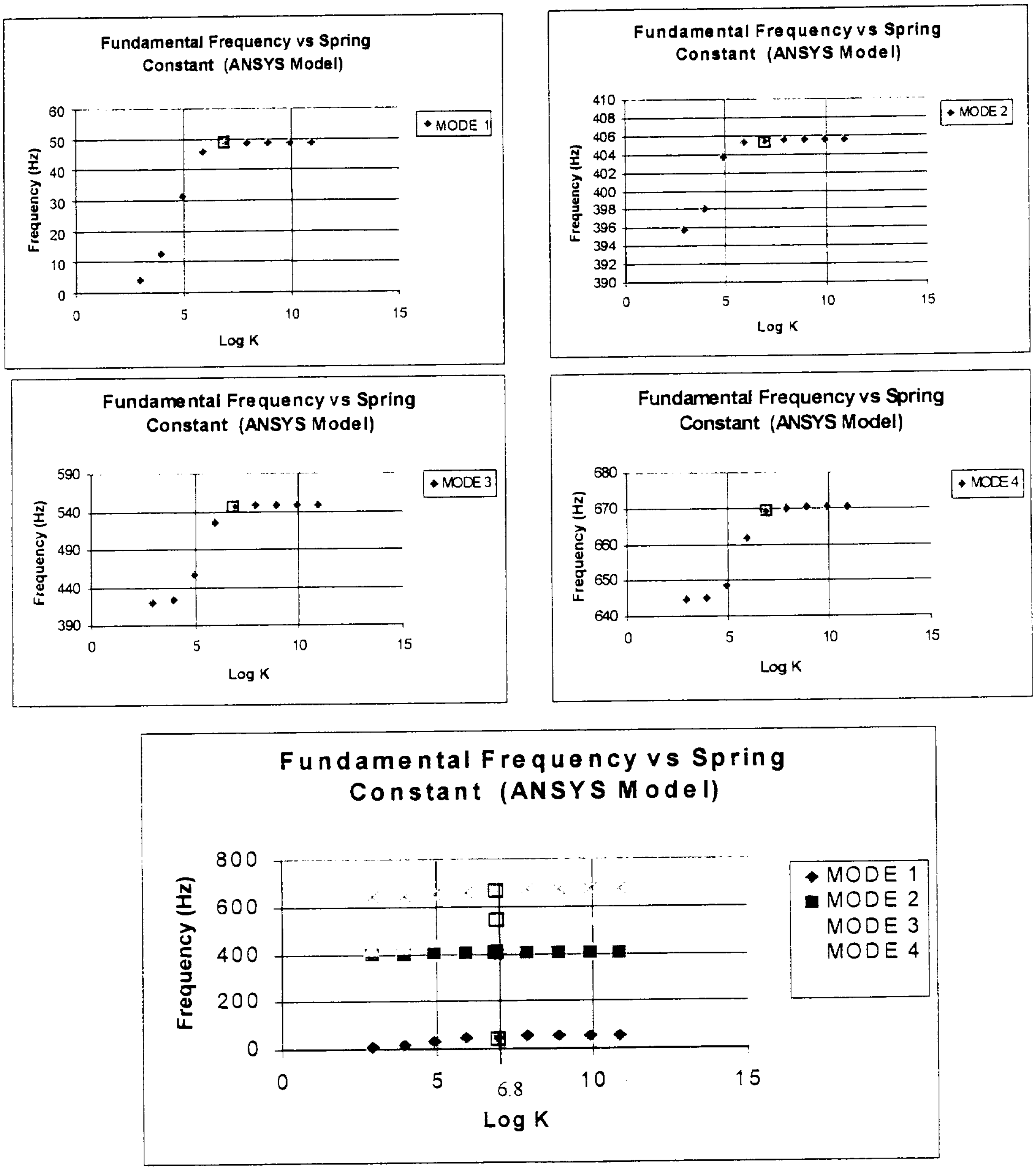

Figure 5. Dependency of torsional mode frequencies to main uncertainty- gear mesh stiffness

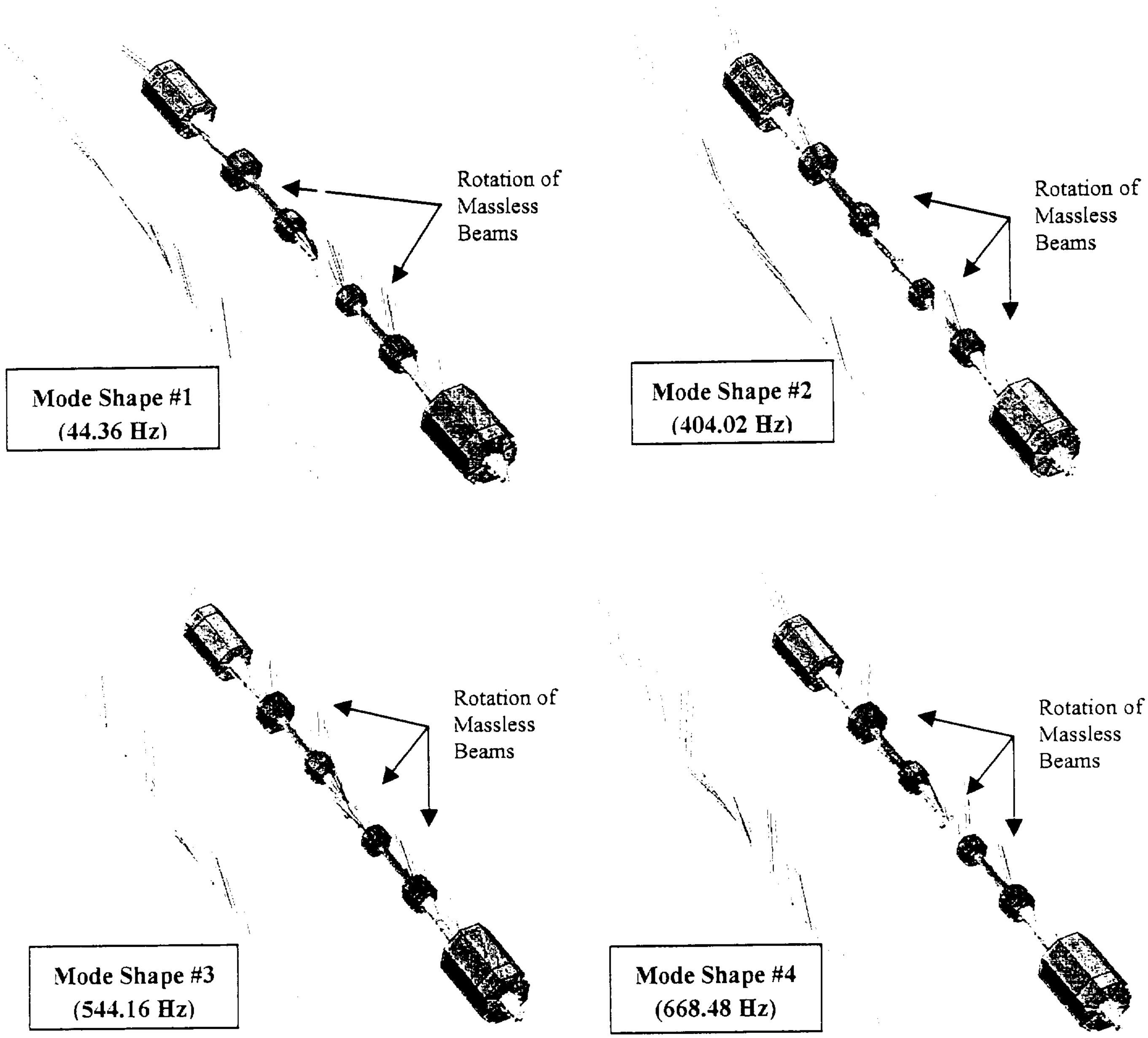

Figure 6. Mode shape analysis shows Modes 1-4 and the predicted frequency of each. Faults that affect torsional stiffness are likely to cause a shift in these frequencies that is detectable and trackable.

The predicted mode shapes are shown above. The models general behavior is reasonable, as there are neither separation points nor odd behavior patterns. For visualization, massless beams, which appear as blue lines perpendicular to the elements, were added to trace the predicted shape of modes 1-4. The nominal linear system mass, stiffness and linear viscous damping are validated through experimental modal analysis to further refine the ANSYS model. This model captures the system-level kinematics and is sensitive to faults that affect stiffness in the torsional domain, such as gear and shaft cracks.

4.1.2. Multiple DOF Model

The complete MDTB lumped parameter system model is being developed using the finite element modeling (FEM) method in corroboration with supporting experimental dynamics analysis. FEM is used to assemble the approximate nominal linear system mass, gyroscopic and stiffness matrices, {M}, {G}, and {K}, and an estimate of the linear system viscous damping, {C}, is produced from experimental modal analysis. The commercial software package ANSYS [Swanson, 1994] is being used to assemble system conservative parameter matrices. A four channel dynamic analyzer, modal impact hammer, the software package STAR MODAL [STAR Users Guide, 1996], and single and triaxial accelerometers are used to perform testing and provide system experimental dynamics information.

In FE models, rotor coupling, shaft, and gear components are modeled employing beam and lumped mass type elements, and gearbox frame/housing and foundation pedestals are modeled employing Plate/Shell and lumped mass and stiffness type elements. Body to body coupling of solid structures in the model has been studied extensively. The inter-body interactions of shaft-bearing-frame [Jones, 1960; Lewis et al., 1965; Lim et al., 1991], bolt-frame [Deutschman et al., 1975; Sun, 1989], coupling-shaft [Moked, 1968; Kirk et al., 1984], and gear-gear [Kahraman et al., 1992; Blankenship et al.; Choy, 1992]) will also be considered.

In order to aid in the validation of lumped parameter characterizations of tachometer/torque transducer and gearbox pedestals, and the system gearbox frame/housing a comparison of experimental obtained mode shape and natural frequencies, and an FE eigenvalue/vector analysis [Choy, 1993; Buckles, 1996] is made with free-free boundary conditions. Also, FE and experimental dynamics tests are performed and evaluated with pedestals in various phases of bolted assembly to aid in the validation and determination of fastener connection parameters.

A two step process will be followed to assure a low order (number of degrees-of-freedom) system model obtains system responses effectively. First, only system component models with a minimal number of finite elements (which simultaneously assure local structural dynamic integrity) is employed, and second, a condensation of portions of the system model (where there is no interest in terms of system response) is used. System matrices are reduced using the Guyan Reduction process [Guyan, 1965; Rouch, 1991] in ANSYS. However, other reduction techniques are available for rotor dynamic systems as well [Mohiuddin, 1998].

4.1.3. Subsystem (Gearbox) Model

System and subsystem models are synthesized to accommodate component natural and critical frequencies from ~ 0 to 4500 Hz. The upper limit being established by anticipated gear transmission error dynamic sideband frequencies that may range up to approximately 4500 Hz (or ~ 5 times the gear mesh frequency of the 3.33 reduction MDTB gearbox operating at 1750 RPM).

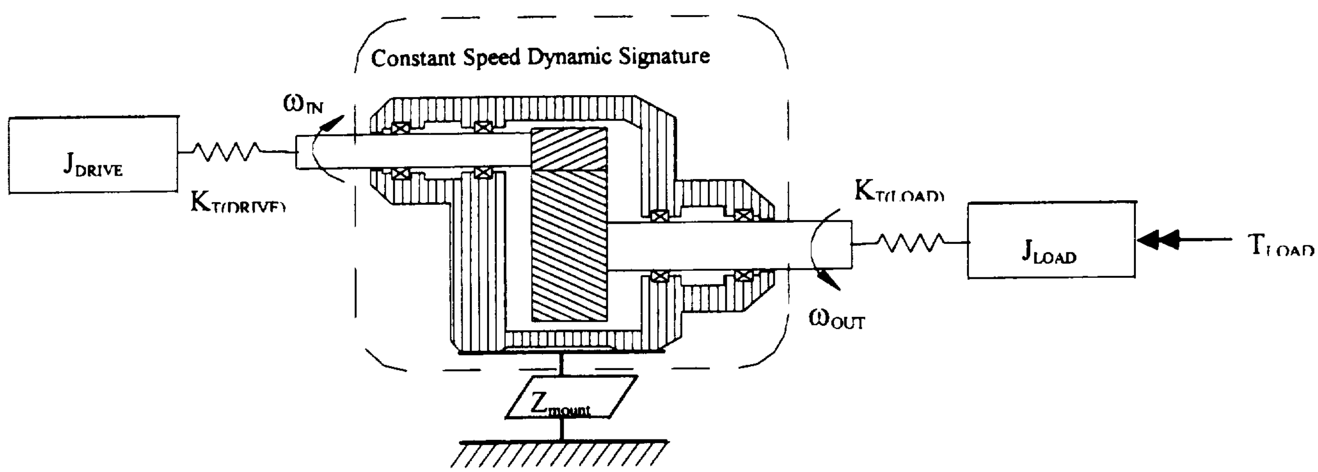

Figure 7. Subsystem gearbox model to associate fault symptoms with gear case measurements will be a finer resolution than system-level model.

As an initial part of all of the six tasks outlined a survey of the critical speeds (due to transverse bending) and mode shapes of all drive train shafts supported on simple bearings (linear spring-damper type) with their associated coupling halves and/or gear disk inertia, and their corresponding torsional and axial natural frequencies, is performed to provide an estimate of the vibratory modes that may participate (due to excitation generated by the 1750 RPM operating condition) in the overall system model. This provides useful data for later synthesis of a complete hybrid system model.

4.2. EXPERIMENTAL CHARACTERIZATION

Initial model related experimental investigation efforts with the MDTB is focused on estimation of the gearbox and tach/torque meter(s) foundation driving point impedances (at their respective mounting fastener points), rotor shaft axial and torsional impedance, and frequency response function background noise measurements. Complex dynamic impedance is estimated from complex effective mass, M, measurements that are estimated by ensemble averaging impact hammer response measurements. Measured frequency response functions are used to initially identify gearbox and tach/torque transducer rotor and foundation natural frequencies and equivalent modal viscous damping parameters. The driveline schematic and planned measurement/load points are shown in

Rotor measurements are made with unidirectional accelerometers and a modal force impact hammer under zero system drive speed, with: zero, one-quarter, one-third, and one-half full normal drive load torque levels. Drive torque is necessary to physically engage the system drive train to assure system: spline coupling, gear-to-gear, and rotor-to-bearing structural continuity. Measurements for driving point impedance are carried out at three locations on the rotor system (One each at the first three shaft couplings starting from the drive motor. These couplings consequently are the only locations that admit access to the assembled rotor system.). Both axial and torsional driving point impedance is necessary with two separate accelerometers for each measurement location. The two separate accelerometer measurements provide discrimination between flexural excited shaft vibrations and the corresponding axial or torsional vibration of interest. The difference of the two response values added to the positive value of the difference is an effective measure of the vibrational degree-of-freedom of interest. Resulting driven point frequency responses are recorded for further analysis.

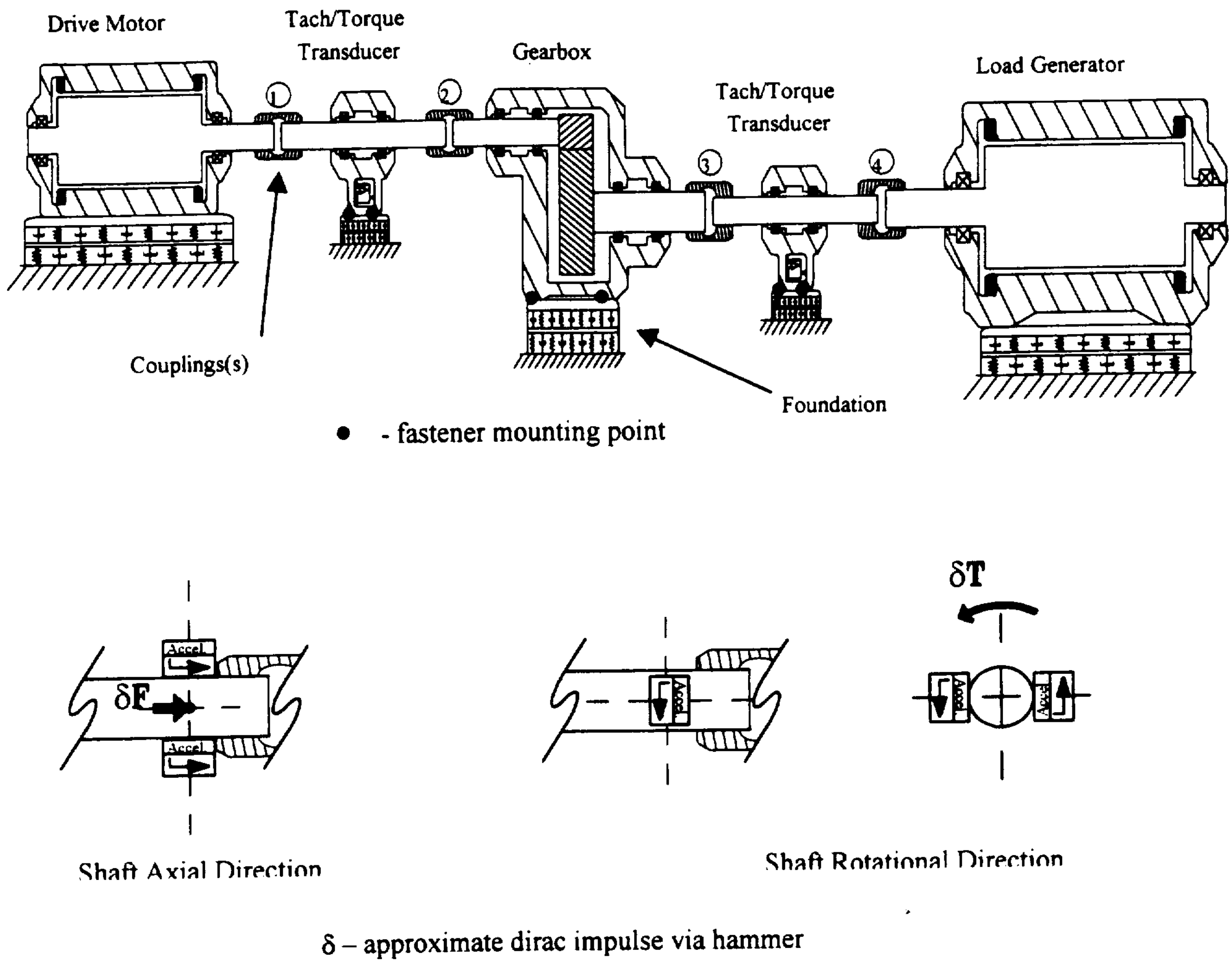

Figure 8. The MDTB driveline and multiple impedance connections for motors and gearbox are shown. The input forces in torsional and axial direction are introduced using impact hammers.

Foundation mounting drive point impedance is made with a triaxial accelerometer (with one axis referenced to the pedestal that is aligned with the gearbox rotor shaft) and a modal impact force hammer, with the corresponding piece of mounted hardware removed. Three MDTB component foundations are assessed (the two tach/torque transducers and the one gearbox pedestal) with a three dimensional driving point frequency response function characterized at each of the mounting point fastener locations on the foundations.

4.3. TRANSITIONAL DATA & STOCHASTIC MODELING

In concert with the Sensing Thrust, we continue to build upon the transitional data collection on the MDTB. During the run-to-failure transitional tests on the MDTB, we collect data from

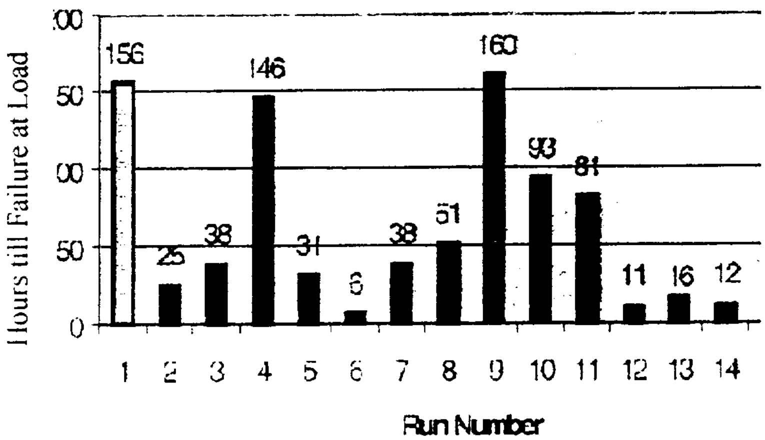

accelerometers, temperature, torque, speed, and oil quality/debris measurements. A summary of current tests and conditions are listed in the following figures. To ground truth the collected data with damage estimates, borescope capability was added to the most recent tests.

Run	Gear Ratio	Run Conditions	Failure Type
[illegible]	[illegible]	Variable	[illegible]
[illegible]	[illegible]	[illegible]	[illegible]
[illegible]	[illegible]	[illegible]	[illegible]
[illegible]	[illegible]	[illegible]	[illegible]
[illegible]	[illegible]	[illegible]	[illegible]
[illegible]	[illegible]	[illegible]	[illegible]
[illegible]	[illegible]	[illegible]	[illegible]
[illegible]	[illegible]	[illegible]	[illegible]
[illegible]	[illegible]	[illegible]	[illegible]
[illegible]	[illegible]	[illegible]	[illegible]
[illegible]	[illegible]	[illegible]	[illegible]
[illegible]	[illegible]	[illegible]	[illegible]
[illegible]	[illegible]	[illegible]	[illegible]
[illegible]	[illegible]	[illegible]	[illegible]
[illegible]	N/A	N/A	N/A
[illegible]	N/A	N/A	N/A

Figure 9. MDTB Run Time History and Failure Summary

The ground truth inspection has allowed us to add an element of stochastic prediction methodology to the MDTB effort. This effort supports selection of inspection interval and decision aiding for crack progression. Each inspection updates the crack growth rate, which could proceed along many paths as is illustrated in Figure 10. Each inspection time allows an update of the model to better isolate the failure trajectory from all possible ones. This capability is show in Figure 11.

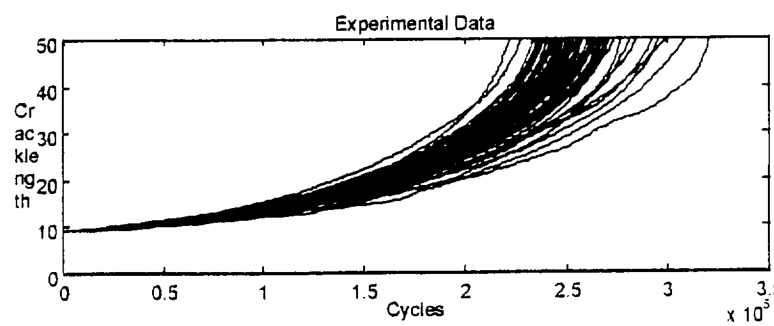

Figure 10. Experimental results from NASA Lewis fatigue data showing distribution of crack growth paths

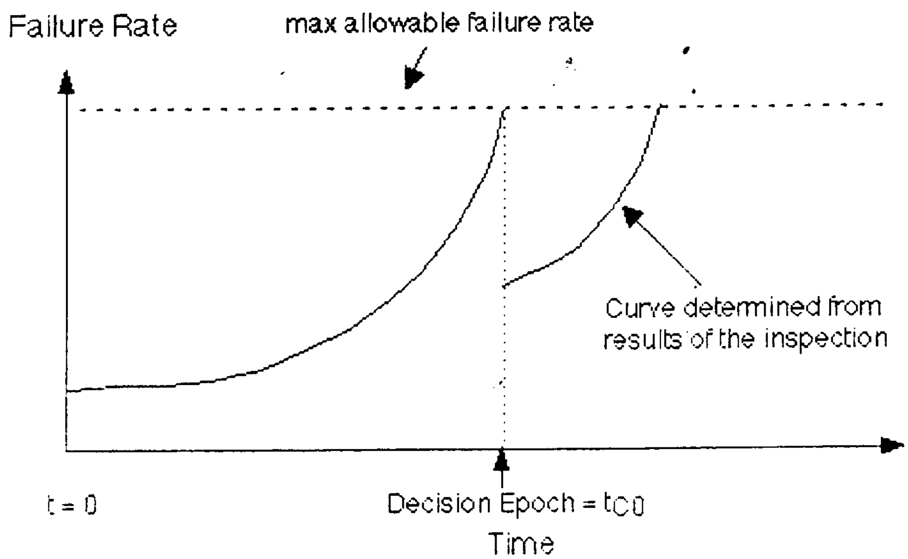

Figure 11. Realization of a failure rate curve after an inspection

The borescope provided excellent visibility to the eye when looking through the eyepiece, but the view through the camera (35mm Nikon) was very dim. The low light level through the camera resulted in 1/2 - 2 second exposure times, which forced the use of a tripod This restricted the ease in which pictures could be taken, due to the need to reposition the tripod for each change of viewing angle. The practice used for this experiment was to visually inspect the interior of the gearbox in detail each time the run was halted, then take a set of pictures of anything of interest, then a set of stock pictures of the gear for archive. Upon stopping a run, the oil inside the gearbox was frothy, and was taken up by the gears and interfered with the pictures. Taking clear shots required waiting for the oil to run off, which took two to three minutes since the oil is highly viscous. Figure 12 is a photo of the driven gear just downstream from the mesh point, taken prior to any damage. As can be seen, the surface of the gear is coated with oil.

Figure 12. Borescope image from test 14 of gear with no damage

The experiment ran for 56 hours at the gearbox's design load, to allow for break-in and any infant mortality that might occur, then was loaded at three times the design load until failure. The run was stopped at the transition from design load to test load for an internal inspection. No visible signs of deterioration were noted. The transition time was 2:00 PM.

Although the run was stopped every two hours for internal inspection, no changes were detected visually until the first gear tooth failure, which occurred just prior to 3:00 AM. An internal inspection had occurred at 2:00 AM, and other than some light scoring of the follower gear's teeth, no major signs of wear were showing. Prior to the 2:00 AM inspection, wavelet analysis of accelerometer data had indicated some possible change, so the 2:00 AM inspection was especially thorough. Still, no visible signs of tooth cracking or spalling were found.

At 3:00 AM. accelerometer data together with a noticeable change in the sound of the gearbox indicated an internal change in the gearbox. The run was stopped at 3:00 AM based on the event noted. Upon inspection, one of the teeth (tooth A) of the follower gear had separated from the gear (Figure 13) The tooth had failed at the root on the motor side of the gear with the crack rising to the top of the gear on the generator side. This was the first indicator that a cracking or spalling of this gear tooth had occurred since the previous inspection

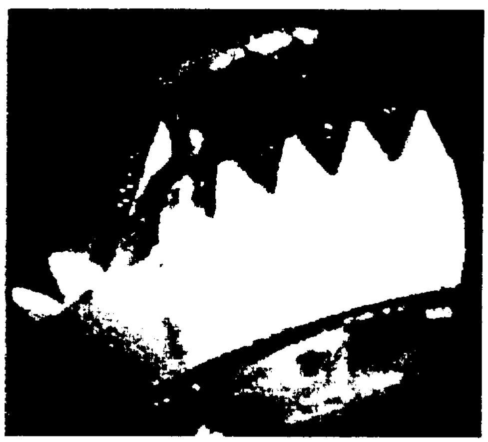

Figure 13. Initial failure: ~9 hours of accelerated loaded portion of the test 14

The anticipation was that the failure would progress rapidly at this point, due to sympathetic failure of the surrounding gear teeth. This was not the case. The run was stopped again at 3:30 AM, and inspection showed no obvious increase in damage. At 5:00 AM, additional wear evident (Figure 14). In this case, another failure mode was detected. The 'downstream' tooth from tooth A (refer to as tooth B) had pieces of its top surface missing, indicating a failure mode of spalling. There were small cracks maybe a millimeter in from the front and rear face of the tooth, parallel to the faces, visible from the motor side of the gear.

Figure 14. Pitting/spalling events can be seen next to initial breakage due to additional surface loading from missing tooth – ~11 hours accelerated loading.

The 7:00 AM inspection showed that the amount of material removed from tooth B had increased, but not excessively. Rather than a runaway failure process, as anticipated, the deterioration was occurring at a steady pace. Neighboring teeth now had material removed from their top-motor side corners, i.e. via spalling. The only visible damage to the driven gear was to tooth A and those within the neighborhood of tooth A (extended to three teeth on either side). There was a significant, noticeable increase in volume and change in the characteristic sound of the gearbox, along with a change in accelerometer data.

On shutdown at 1100 AM, with a significant increase in vibration, eight teeth suffered damage. The damaged teeth were dispersed in clusters around the gear. It appears that there were independent clusters of failure processes, within each cluster there was a tooth failed due to root cracking surrounded by teeth failing due to spalling. Figure 15 is a picture showing two of the clusters close to each other. Both clusters have the upstream tooth failed by cracking at the root, and the following tooth showing evidence of spalling.

This ground truth observation has offered several insights into the failure process. The change that occurred in the wavelet analysis results prior to the 2:00 AM inspection, and before any observable changes in the gears were evident, indicates that the wavelet analysis holds promise for detecting impending failures of gear teeth. The gear tooth failure process exhibited of a steady sequence of small failures, even at 3X loading, as opposed to one small failure leading to a catastrophic sympathetic chain reaction failure. Based on this observation, it would appear that gear failure is due to a number of independent processes around the gear. Each independent process consisting of an initial tooth failure due to fatigue cracking, and sympathetic tooth failures of the downstream teeth due to spalling. It is important to note that on shutdown, the gear was still turning torque and RPM into torque and RPM, i.e. its ability to perform its function had not markedly suffered. So by some measures, it had not yet failed. Taken with the previous lesson learned, it reasonable to state that gear failure is preceded by macroscopically observable deterioration, which itself is preceded by precursors detectable through wavelet analysis.

From the perspective of borescope equipment, the strength of the light source is critical. A video camera type of capture mechanism is needed. With regard to the MDTB, a mechanism for removing the oil from gear teeth, such as compressed air, is necessary to provide the best view of the gear.

Figure 15. An image at shutdown indicates pitting and tooth breakage in many locations – 16 hours cumulative accelerated loading

For reference to processed feature data, *Figure 16* shows an interstitial enveloping of gearbox accelerometer data from the run. It illustrates clear areas of activity that directly correlate to the gear tooth failure and appears to be tracking the fault well. The ability to track the damage and ground truth the data with borescope images is key to interpreting signatures. The dynamic models hold promise for interpreting these data and identifying response observables that can be used for predictive diagnostics.

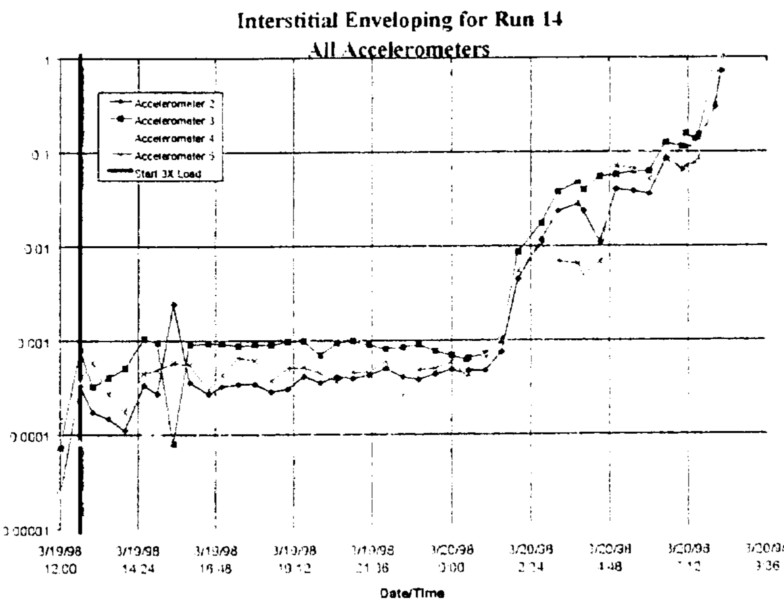

Figure 16. Interstitial Processing of Run 14 showing effects of damage

5. REVIEW OF CONTINUING WORK

Work is planned to continue in all reviewed areas in this report. The computational modeling effort will investigate higher degree of freedom subsystem and system level models that are based upon impedance and stiffness inputs from the experimental efforts. Adaptation of working models will feed into the power flow analysis of the driveline. Torsional and axial measurements collected during the transitional failure runs will be analyzed to correlate failure effects on structural response and power flow observables. The predictive modeling using non-linear methods will be further developed on additional sensors and other identified features. We will also continue to investigate methods to integrate the fault effects into predictive models.

6. REFERENCES

1. Badgley, R.H., Fleming, D.P., and Smalley, A.J., 1974, *Drive-Train Dynamics Technology: State-of-the-Art and Design of a Test Facility for Advanced Development*, ASME Paper No. 75-DET-74.
2. Byington, C. S. and Kozlowski, J. D., 1997, *Transitional Data for Estimation of Gearbox Remaining Useful Life*, 51st Meeting of the Society for Machinery Failure Prevention Technology (MFPT).
3. Dimentberg, F. M., 1961, **Flexural Vibrations of Rotating Shafts**, Butterworths, London, England
4. Tondl, A., 1965, **Some Problems of Rotor Dynamics**, Publishing House of the Czechoslovak Academy of Sciences : Chapman & Hall, London, England
5. Dimarogonas, A.D., 1983, **Analytical Methods in Rotor Dynamics**, Applied Science Publishers, London, England.
6. Rao, J.S., 1983, **Rotor Dynamics**, Halsted Press, J. Wiley, New York.
7. Vance, J.M., 1988, **Rotordynamics of Turbomachinery**, John Wiley and Sons, New York
8. Childs, D.W., 1993, **Turbomachinery Rotordynamics, Phenomena, Modeling, and Analysis**, J. Wiley, New York.
9. Kramer, E., 1993, **Dynamics of Rotors and Foundations**, Springer-Verlag, New York.
10. Lee, C-W, 1993, **Vibration Analysis of Rotors**, Kluwer Academic Publishers, Boston.
11. Dudley, D.W., 1994, **Handbook of Practical Gear Design**, Technomic Publishing, Lancaster, PA.
12. LaLanne, M. and Ferraris, G., 1998, **Rotordynamics Prediction in Engineering**, 2nd Ed, John Wiley and Sons, Chichester, England.
13. Mitchell, L.D., and Daws, J.W., 1982, *A Basic Approach to Gearbox Noise Prediction*, SAE Paper 821065, Society of Automotive Engineers, Warrendale, PA.
14. Ozguven, H.N., and Houser, D.R., 1988, *Dynamic Analysis of High Speed Gears, by Using Loaded Static Transmission Error*, Journal of Sound and Vibration, V. 125, n. 1, pp. 71-83.
15. Choi, M., and David, J.W., Mesh Stiffness and Transmission Error of Spur and Helical Gears, 1990, SAE Paper 901764, Society of Automotive Engineers, Warrendale, PA.
16. Lim, T.C., and Singh, R., 1991, *Vibration Transmission through Rolling Element Bearings. Part III: Geared Rotor Systems Studies*, Journal of Sound and Vibration, V. 151, n. 1, pp. 31-54.
17. Kahraman, A., 1993, *Effect of Axial Vibrations on the Dynamics of a Helical Gear Pair*, ASME Journal of Vibration and Acoustics, V. 115, pp. 33-39.
18. Rao, R.K.N. (editor), 1996, **Handbook of Condition Monitoring**, 1st edition, Elsevier Advanced Technology, Oxford, UK.
19. Randall, R.B., 1982, *A New Method of Modeling Gear Faults*, Transactions of the ASME, Journal of Mechanical Design, V. 104, pp. 259-267.

20. McFadden, P.D., and Smith, J.D., 1986, *A Signal Processing Technique for Detecting Local Defects in a Gear from the Signal Average of the Vibration*, Proceedings of the Institution of Mechanical Engineers, V. 199, n. C4.

21. Nelson, H.D., and Nataraj, C., 1986, *The Dynamics of a Rotor System with a Cracked Shaft*, ASME Journal of Vibration, Acoustics, Stress, and Reliability in Design, V. 108, n. 2, pp. 189-196.

22. Wauer, J., 1990, *On the Dynamics of Cracked Rotors: A Literature Survey*, ASME Applied Mechanics Reviews, V. 43, n. 1, pp13-17.

23. Wauer, J., 1990, *Modelling and Formulation of Equations of Motion for Cracked Rotating Shafts*, International Journal of Solids and Structures, V. 26, n. 8, pp. 901-914.

24. Jun, O.S., Eun, H.J., Earmme, Y.Y., and Lee, C-W, 1992, *Modelling and Vibration Analysis of a Simple Rotor with a Breathing Crack*, Journal of Sound and Vibrations, V. 155, n.2, pp. 273-290.

25. Dyer, D., and Stewart, R.M., 1978, *Detection of Rolling Element Bearing Damage by Statistical Vibration Analysis*, Transaction of the ASME, Journal of Mechanical Design, V. 100, pp. 229-235.

26. Braun, S., and Datner, B., 1979, *Analysis of Roller/Ball Bearing Vibrations*, Transactions of the ASME, Journal of Mechanical Design, V. 101, pp. 118-125.

27. McFadden, P.D., and Smith, J.D., 1984, *Model for the Vibration Produced by a Single Point Defect in a Rolling Element Bearing*, Journal of Sound and Vibration, V. 96, n. 1, pp. 69-82.

28. Swanson Analysis Systems, 1994, ANSYS User's Manual for Revision 5.0, Volume IV, Theory, Swanson Analysis Systems, Houston, PA .

29. STAR System Users Guide (P/N 3405-0113), 1996, Spectral Dynamics Inc., San Jose, CA

30. Jones, A.B., 1960, *A General Theory for Elastically Constrained Ball and Radial Roller Bearings Under Arbitrary Load and Speed Conditions*, Transaction of the ASME, Journal of Basic Engineering, V. 82, pp. 309-320.

31. Lewis, P., and Malanoski, S.B., 1965, Rotor-Bearing Dynamics Design Technology, Part IV: Ball *Bearing Design Data*, AD 466393, Air Force Aero Propulsion Laboratory Research and Technology Division, Wright-Patterson Air Force Base, Ohio.

32. Lim, T.C., and Singh, R., 1991, *Vibration Transmission through Rolling Element Bearings. Part I: Bearing Stiffness Formulation*, Journal of Sound and Vibration, V. 139, n. 2, pp. 179-199.

33. Deutschman, A.D., Michels, W.J., and Wilson, C.E., 1975, **Machine design, Theory and Practice**, Sec. 16-10, MacMillan Publishing, New York.

34. Sun, W., 1989, Bolted Joint Analysis using ANSYS Superelements and Gap Eleements, 1989 ANSYS Conference Proceedings, pp. 6.66-6.75, Swanson Analysis Systems, Houston, PA.

35. Moked, I., 1968, *Toothed Couplings-Analysis and Optimization*, Transaction of the ASME, Journal of Engineering for Industry, pp. 425-434.

36. Kirk, R.G., Mondy, R.E., and Murphy, R.C., 1984, *Theory and Guidelines to Proper Coupling Design for Rotor Dynamics Considerations*, ASME Journal of Vibration, Acoustics, Stress, and Reliability in Design, V. 106, pp. 129-138.

37. Kahraman, A., Ozguven, H.N., Houser, D.R., and Zakrajsek, J.J., 1992, *Dynamic Analysis of Geared Rotors by Finite Elements*, ASME Journal of Mechanical Design, V. 114, pp. 114-514.